ISSN 0024-4902, Lithology and Mineral Resources, 2006, Vol. 41, No. 2, pp. 137–164. © Pleiades Publishing, Inc., 2006.
Original Russian Text © V.Yu. Lavrushin, V.N. Kuleshov, O.E. Kikvadze, 2006, published in Litologiya i Poleznye Iskopaemye, 2006, No. 2, pp. 154–182.

Travertines of the Northern Caucasus

V. Yu. Lavrushin, V. N. Kuleshov, and O. E. Kikvadze

Geological Institute, Russian Academy of Sciences (GIN),
Pyzhevskii per. 7, Moscow, 119017 Russia
e-mail: v_lavrushin@ginras.ru

Received June 27, 2005

Abstract—Mineralogical and isotope-chemical characteristics of carbonate travertines of the Greater Caucasus are investigated. It is shown that concentrations of many chemical elements, which predominantly precipitate together with iron hydroxides, decrease along the strike of the travertine dome. At the same time, $\delta^{13}C$ and ^{18}O values in carbonates systematically increase due to kinetic effects of isotope fractionation. This leads to the formation of isotopically heavy calcite ($\delta^{13}C$ up to 16.3‰) near the travertine dome base. Concentrations of other elements (Mg, Sr, Ba, Na, S, and Li), which form a isomorphic part of calcite crystal lattice, almost do not change along the strike of the dome. Comparison of concentrations of these elements in travertines and initial water solutions makes it possible to get ideas on trends of their redistribution in the carbonate–water system. Correlations found in this work define not only TDS content and concentration of some ions, but also REE spectra and formation temperatures of ancient fluid systems.

DOI: 10.1134/S0024490206020040

Travertines (or calcareous tufas) are carbonate sediments formed in places of groundwater discharge. They are most frequently encountered in the fields of development of cold and thermal CO_2-rich (sometimes with N_2) mineral waters.

Travertines are of interests from different points of view. It is known that cold and thermal CO_2-rich and N_2- and CO_2-rich waters are related to mobile belts of the Earth, i.e., to the regions with high activity of tectonomagmatic processes (Disler, 1971). Therefore, the findings of travertine domes or their fragments in ancient sediments can mark the periods of tectonomagmatic activation. Travertine accumulations can also be considered a source of information about paleoseismic events that are not recorded by other methods (Disler and Avtandilova, 1991; Zilberman *et al.,* 2000). During strong earthquakes, fractures and displacements appear on the surface of travertine cones. After the earthquake, mineral spring vents frequently change their position, giving rise to new travertine domes. Investigation of travertines also allows us to reconstruct the chronology of paleoclimatic events (Poage *et al.,* 2000).

However, travertines are most interesting as the basis for paleohydrogeological reconstructions. They form predominantly by the chemogenic process. Therefore, we can expect that they inherit some chemical and isotopic ($\delta^{13}C_{CO_2}$ and $\delta^{18}O_{H_2O}$) peculiarities of the initial gas–water solutions. The fluid regime can vary with time (we understand the term "fluid regime" as a complex of physicochemical characteristics of gas–water fluid (chemical and isotopic compositions of waters and gases, temperature of water formation, and so on) that can change depending on conditions of fluid circulation in the Earth's crust). In this case, travertines (and, possibly, vein bodies as well) remain the unique sources of information about ancient fluids. However, in order to use travertines in this capacity, we should know the pattern of redistribution of chemical elements in the travertine–water system and the scale of natural variations in their isotope-chemical composition along the strike of travertine dome.

Travertines of mineral waters in the Greater Caucasus were studied just from these positions.

MATERIALS AND METHODS

More than 40 recent travertine domes are known in the Greater Caucasus. In the central sector of this mountain system, all travertine domes are related to issues of CO_2-rich waters; at the periphery (eastern and western Caucasus and Kura Basin), to the discharge of methane- and CO_2-rich fluids. The majority of travertine-accumulating springs are formed in Paleozoic and Mesozoic sediments (Fig. 1, Table 1). Travertines are seldom found at outcrops of Lower Paleozoic crystalline rocks in the core of the Greater Caucasus. They are more frequently confined to Paleozoic–Mesozoic sedimentary and volcanosedimentary complexes.

In general, areas of travertine domes in the Greater Caucasus are small (from tens to a few hundreds of square meters). The largest domes are known on the northern slope of the Greater Caucasus near Pyatigorsk (on slopes of Mt. Mashuk), in the vicinity of the Elbrus Volcano (Upper Tokhana Spring and Upper Baksan Settlement), near the Kazbek Volcano (Upper Karma-

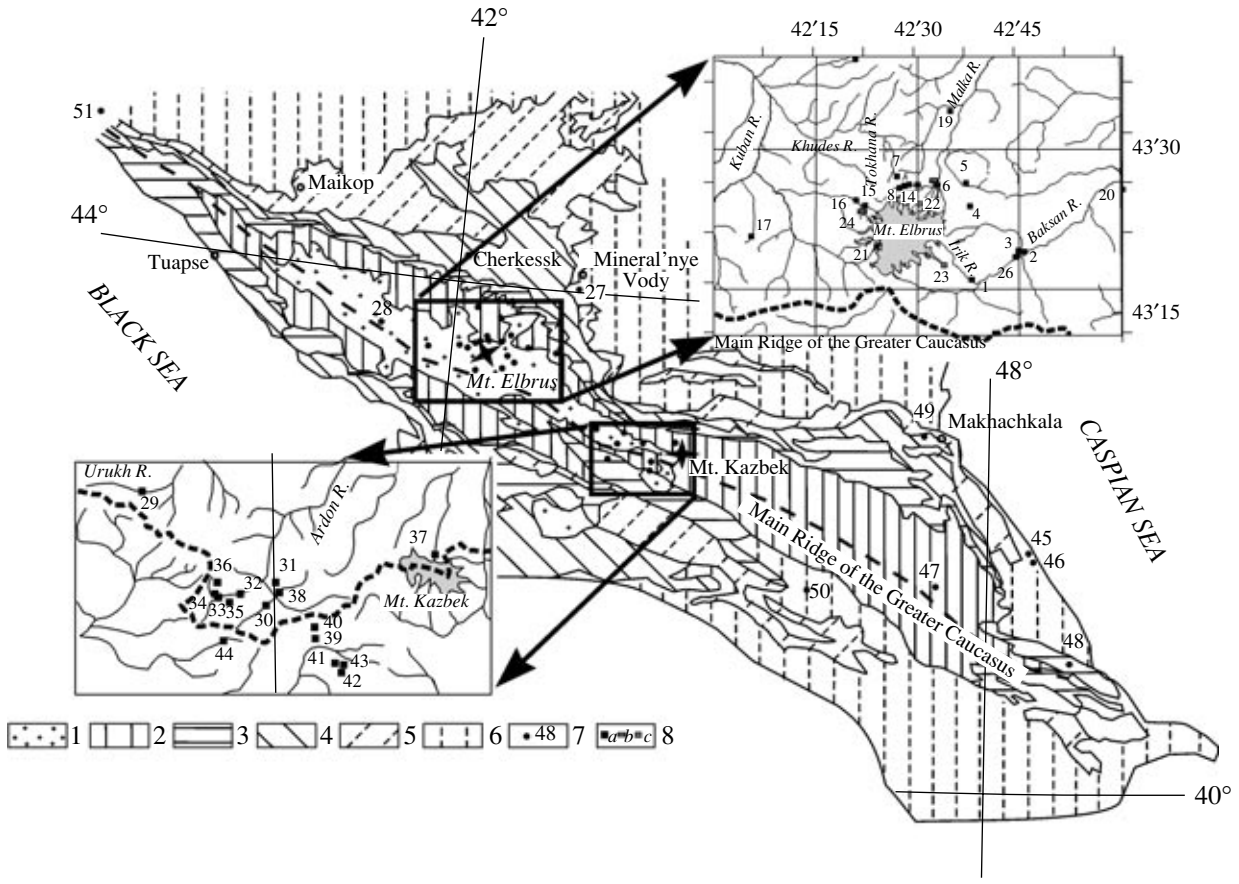

Fig. 1. Distribution of travertines in the Greater Caucasus. (1) Outcrops of Paleozoic basement; (2–6) rock complexes: (2) Jurassic, (3) Cretaceous, (4) Paleogene, (5) Neogene, (6) Quaternary; (7) sites of travertine sampling; (8) sites of sampling (in insets): (*a*) travertines, (*b*) carbonate veins and limestones, (*c*) opalites.

don springs), and in Lashtrak (Pkhei or Kislye) spring area situated at upper reaches of the Bol'shaya Laba River. On the southern slope, large travertine domes are observed on the Kel'sk volcanic plateau (Suna and Britata springs).

In total, we investigated 37 mineral springs that accumulate travertines. Coordinates of the majority of sampling sites are given in Table 1. We also studied 21 samples of old travertines. A part of these samples was taken from ancient domes (in situ). Another part was taken from alluvial, terminal moraine, and slope deposits. The last group includes not only clastic carbonate travertines, but also hydrothermally altered rocks (opalites) an insignificant admixture of carbonates. For the sake of comparison, we also studied several fragments of carbonate veins from granite gneisses of the Main Ridge and Upper Cretaceous limestones of the eastern Caucasus.

Chemical composition of travertines was determined in acidic extracts by plasma mass spectrometry (ICP-MS) with a PlasmaQuard device (VG, Great Britain) and plasma-emission spectrometry (ICP-AES) with an ICAP-61 device (Thermo Jarrel Ash, United States) at the Institute of Microelectronic Technology and Ultrahigh-Purity, Russian Academy of Sciences (IPTM, Chernogolovka). The acidic extract was prepared by dissolving weighed samples of ground carbonate (200 mg) in hot 10% hydrochloric acid. The weight of insoluble residue was recorded. It should be noted that not only calcium carbonates, but also iron hydroxides are transferred to the solution in this procedure.

The $\delta^{13}C$ and $\delta^{18}O$ values in $CaCO_3$ were determined in the same samples. CO_2 was separated in accordance with the standard method (McCrea, 1950) in orthophosphoric acid (H_3PO_4). The isotopic composition was determined with a MI-1201V mass spectrometer. The accuracy of $\delta^{13}C$ and $\delta^{18}O$ determinations was 0.25‰. The $\delta^{13}C$ and $\delta^{18}O$ values are given in ‰ relative to the PDB and SMOW standards, respectively.

The chemical composition of travertine-depositing waters was also studied. The pH values, Cl and HCO_3 concentrations, and dry residue were determined in line with standard methods. Concentrations of the remaining components were determined in water samples con-

Table 1. Coordinates of some sites of travertine sampling

No. in Fig. 1	Sample no.	Mineral springs (sampling site)	N°	E°	Altitude, m
		Elbrus area			
1	8-2/01	Irik-narzan Spring	43.26392	42.63558	2100
2	176/99	Upper Baksan Settlement, nizhii narzan	43.31514	42.75667	1575
26	10/01	Upper Baksan Settlement, upper narzan	43.30444	42.73894	1538
6	17/98	Malka River, narzan	43.43344	42.47092	2200
7	T-2/01	Tokhana River, Upper Tokhana narzan	43.46864	42.44283	2709
10	K3/00	Kizilkol River, right bank, old travertine	43.43697	42.47889	2813
11	K4/00	Kizilkol River, right bank, well	43.43344	42.47092	2674
12	K5-1/00	Kizilkol River, right bank, old travertine	43.43536	42.47031	2804
13	K6/00	Kizilkol River, right bank, old travertine	43.43281	42.46414	2820
14	K7/00	Kizilkol River, right bank, narzan	43.43772	42.49981	2686
15	4/98	Biitiktebe River, upper narzan in riverbed, 200 m upstream of Dzhilysu	43.40372	42.35222	2632
16	7/98	Biitiktebe River, narzan, about 2.5 km downstream of Dhzilysu	43.41661	42.31317	2300
17	22/01	Uchkulanichi River, narzan in upper reaches	43.36089	42.09708	2515
18	17/01	Amankol River, old aragonite nodule	43.68072	42.25036	1700
19	20/00	Ingushli River, Lower Ingushli narzan	43.52875	42.52767	1997
20	7/01	Gerkhodzhan River, right tributary of Baksan River (Tyrnyauz area), old travertine	43.37364	42.95506	~1500
21	148-4*	Ullu-Kam River, upper reaches, travertine from terminal moraine	43.31814	42.39025	3130
		Opalites (Elbrus area)			
22	o-1/00	Kizilkol River, opalite fragment from alluvium	43.40286	42.48317	2900
23	o-2/00	Terminal moraine of the Terskol Glacier, opalite fragment	43.30383	42.50964	3259
		Northwestern Caucasus (upper reaches of the Verkhnyaya Laba River)			
28	29-2/01	Pkhiya River (Lashtrak and Kislye springs)	43.47906	40.91536	1860
		Northern Ossetia			
29	23/99	Tanadon River, right tributary of the Urukh River, Kubus narzan	42.88311	43.59433	2061
30	33/00	Zrug-don River, Khasiev Spring	42.59369	44.00783	1805
31	33-1/00	Tsmiakom-don River (right tributary of the Ardon River), narzan	42.69622	43.99656	1785
32	35/00	Well Tib 1	42.67536	43.92403	1772
33	8/03	Chel'diev narzan	42.65000	43.81231	2069
34	9/03	Karta Spring	42.64917	43.80286	2206
35	10/03	Lower Zgil Spring	42.65406	43.82092	2058
36	13/03	Bubu Spring	42.67547	43.80519	2347
37	38-1/00	Upper Karmadon springs (CO_2-rich)	42.75469	44.48094	2330
		Southern Ossetia			
39	18-03	Sba Spring	42.57242	44.17303	1752
40	19-03	Suna Spring	42.60647	44.18986	2045
41	26-03	Lower Britata Spring (on the left bank)	42.52058	44.19461	1862
42	27-03	Upper Britata Spring (on the right bank)	42.50631	44.19025	1942
43	28-03	Middle Britata Spring (on the right bank)	42.51783	44.19761	1870
44	31-03	Kesel'ta Spring	42.48064	43.92644	1101
		Eastern Caucasus (Dagestan)			
45	135/90	Thermal spring in the Adzhi Channel	42.33303	48.08553	–15
46	206/02	Berikei, Well 10 (A. Nobel)	42.25825	48.11861	–9
47	229/02	Kuan narzan, left bank of the Andiiskii Koisu River	42.40633	45.94975	1312
48	217/02	Left tributary of the Samur River, Chakh-Chakh Spring area, outcrop of old travertines	41.51017	48.09172	718
49	D6/02	Quarry near the Talgi Settlement, carbonate vein in Upper Cretaceous limestones	42.86661	47.46003	150

Note: *Sample presented by V.M. Gazeev. The Caucasian term "narzan" designates "vigorously bubbling spring."

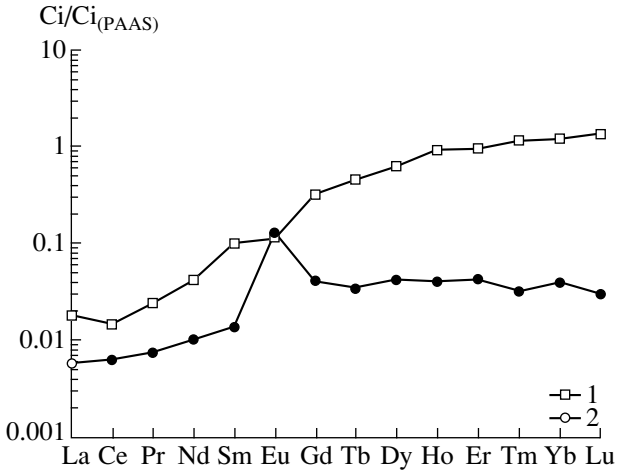

Fig. 2. PAAS-normalized REE distribution in CO_2-rich waters of the Greater Caucasus. (1) Typical spectrum characterized by the growth of HREE concentrations (Uchkulanichi Spring no. 17); (2) spectrum with prominent Eu maximum (Irik-narzan Spring no. 1).

served with the nitric acid by the ICP-MS and ICP-AES methods in the chemical laboratory of the IPTM.

During the analysis of chemical compositions of travertines versus water interrelations, data on mineral waters and travertines from eastern Chukotka were also examined for the sake of comparison. In contrast to travertines of the Greater Caucasus, their counterparts in eastern Chukotka are formed exclusively from thermal waters (*T* from ~20 to 95°C) (Cheshko *et al.,* 2004; Polyak *et al.,* 2004). These data permit the appraisal of the role of regional factors (temperature and salt composition) in the correlation of compositions of waters and travertines.

GENERAL DESCRIPTION OF TRAVERTINE-DEPOSITING MINERAL SPRINGS OF THE GREATER CAUCASUS

In the Greater Caucasus, approximately 300 CO_2-rich springs are known, but carbonates are precipitated in only a minor part of them (about 40). Almost all of the springs are cold (4–15°C). Higher temperatures (50–60°C) are noted only in the Verkhne-Karmadon (northern slope of the Kazbek Volcano) and Proval springs (Mt. Mashuk in the Caucasian Mineral'nye Vody area).

The travertine-depositing CO_2-rich waters have a variable composition (*Uglekislye…*, 1963). Their TDS content changes from 1.5 to 12.9 g/l (average 2–4 g/l). These waters belong to HCO_3–Ca, more rarely Cl–HCO_3–Na–Ca types. Waters of travertine domes are distinguished from other CO_2-rich springs of the Greater Caucasus by higher concentrations of potassium (more than 200 mg/l) (Table 2).

Despite a relatively low TDS content, mineral waters of the Caucasus often contain high concentrations of the following elements: Li, Be, Fe, B, Si, Sr, Ba, and As (Lavrushin *et al.,* 2003a). Concentrations of rare earth elements in the waters are very low (frequently, below the limit of detection by the ICP-MS). Therefore, we can judge about their complete spectra only on the basis of separate analyses. The majority of REE spectra are rather uniform. They are characterized by relatively higher concentrations of HREE. The growth of concentration usually starts with Sm and Eu and continues up to Lu (Fig. 2). In general, these spectra are typical of waters saturated with carbon dioxide (Balashov, 1976).

However, REE distribution in waters from Irik-narzan no. 1 (hereafter, numbers of springs correspond to those in first columns of tables and in Fig. 1), Upper Tokhana no. 7, Sba no. 39, and Sunna no. 40 are distinguished by high Eu concentrations (Fig. 2). In contrast to other REEs, Eu can pass into bivalent state under reductive conditions and become more mobile. Therefore, one can expect that waters of these springs formed under highly reductive conditions, possibly, at the presence of H_2S. The other possible reason is leaching of Eu from Neogene–Quaternary volcanogenic rocks that crop out in the immediate vicinity of these springs.

MORPHOLOGICAL AND MINERALOGICAL ZONATION OF TRAVERTINE BUILDUPS

The travertine domes represent a complex interrelation of chemogenic and biogenic formations. The chemogenic sediments are represented by carbonates and iron hydroxides; the biogenic ones, by colonies of blue-green and diatom algae. Travertines also often contain fragments of terrestrial plants (moss, tree leaves, and grass stems).

Carbonates and iron hydroxides are not simultaneously precipitated from mineral waters. Therefore, a certain mineralogical zonation is formed in sediments of travertine-depositing springs. Let us consider its peculiarities with travertine domes of the Upper Tokhana Spring (no. 7) as an example. Here, we can distinguish four consecutive zones located at different distances from the outlet of mineral waters on the surface.

Zone of intense ferrugination (A) is confined to the center of mineral water discharge and extends over a few tens of meters. The zone is characterized by intense precipitation of amorphous iron hydroxides that impart bright red-brown color to the discharge area.

Carbonates in this zone sporadically form only along the coastline or on stones rising above the level of mineral water. The thickness of carbonate crust does not exceed a few millimeters. The crust includes not only fine- and microcrystalline calcite, but also spicular crystals of aragonite that sometimes form radiate-fibrous aggregates. They fill pores and caverns in carbonate crusts left after decayed algae (Fig 3a). Colonies

Table 2. Chemical composition of CO_2-rich travertine-depositing springs in the Greater Caucasus

No.in Fig. 1	Sample no.	Name of spring	*T*, °C	pH	Total, g/l	HCO_3, mg/l	Cl, mg/l	Li, μg/l	Be, μg/l	B, μg/l	Na, μg/l	Mg, μg/l	Al, μg/l	Si, μg/l	S, μg/l	K, μg/l	Ca, μg/l
1	8/01	Irik-narzan Spring	10.0	6.16	2.3	1435	184	1079	2.8	15254	236648	88115	59.6	17559	40570	16290	218093
1	8-4/01	Irik-narzan, 12 m downslope of the spring	–	–	1.9	1148	184	1009	0.23	14390	234279	83221	165	16231	36533	15648	186896
2	9/01	Upper Baksan Settlement, lower narzan	17.2	6.36	5.5	2584	1075.6	13532	3.2	140282	883300	96439	115	18922	87279	85747	342995
26	10/01	Upper Baksan Settlement, upper narzan	14.1	6.06	2.8	1364	205.9	3528	1.1	36247	306271	124199	219	24144	162897	37259	245578
5	24/00	Lower Shaukol Spring	4.4	5.67	0.67	439	49	127	0.11	1500	46681	26325	150	9127	5315	3366	81935
7	14/01	Upper Tokhana Spring	6.6	6.27	2.1	1256	10.6	6.7	0.1	135	7037	34527	139	5544	122150	564	370187
7	14-15/01	Upper Tokhana, 250 m downslope of the spring	–	–	1.1	390	5.3	4.5	0.10	45.8	7304	35679	215	5733	131776	742	359615
11	K-4/00	Well on the Kizilkol River	9.6	5.55	1.40	1037	39.7	176	0.65	2050	62740	45870	203	–	9404	1589	251816
14	K-7/00	Kizilkol River, narzan on the right bank	8.6	6.07	2.01	1525	5.7	18.1	0.30	707	16660	30249	13.1	17674	1877	1599	502684
15	4/98	Biitiktebe River, narzan	9.6	5.8	2.33	1342	318	1897	3.8	18070	453700	58430	154	–	6860	48520	95807
16	7/98	Biitiktebe River, narzan	9.5	5.68	2.68	1506	426	2307	5.5	35260	505000	60710	161	–	245	45320	184029
17	22/01	Uchkulanichi, narzan	2.4	6.36	3.97	2488	372	860	30.1	22357	517400	168198	771	21410	25262	8414	354260
19	20/00	Lower Ingushli Spring	10.1	6.22	3.82	1903	744	2350	2.2	34005	1639489	65348	25.7	6360	10697	40499	123459
28	29-2/01	Lashtrak narzans, Svyatoi Spring	10.0	5.77	2.09	1372	159	168	<0.1	19817	290300	13580	165	16043	5977	4917	276462
28	29-1/01	Lashtrak narzans, vent 2	16.0	6.54	4.48	2684	514	490	<0.1	62393	1017600	29680	271	27540	6267	13994	525537
29	23/99	Kubus Spring, Urukh River	5.6	6.3	5.30	2056	1588	7051	4.2	145170	961629	70554	45.6	11250	3629	89432	399942
33	8/03	Chel'diev Spring	8.4	6.1	1.59	1159	17.7	75.3	0.14	2511	72234	32958	53.0	4039	5921	2755	309600
34	9/03	Karta Spring	7.1	6.24	3.05	2288	17.7	86.6	0.83	1249	50905	35325	77.3	10756	317	2486	730822
35	10/03	Lower Zgil Spring	8.4	6.28	3.21	2379	56.7	562	<0.1	11201	657403	55591	109	6226	7748	12106	334600
36	13/03	Bubu Spring	5.3	5.97	2.07	1586	14.2	26.0	0.14	379	23491	41146	28.8	4240	7032	1373	417200
37	4/03	Upper Karmadon Spring	41.9	6.17	5.87	732	2872	9605	0.87	50076	2102621	42667	77.8	21826	30601	205612	323000
39	18/03	Sba Spring	8.2	6.37	4.46	2830	326	1341	1.2	22498	1117469	48770	73.4	5133	13892	8517	167259
40	19/03	Suna Spring	12.2	6.24	2.53	1723	42.5	302	0.37	4331	104870	84501	68.6	4019	27047	1856	493800
41	26/03	Lower Britata Spring	8.2	6.07	2.00	1464	42.5	198	0.22	3962	121017	30634	24.9	4764	9342	2007	389800
42	27/03	Upper Britata Spring	8.4	6.16	2.78	2074	78	644	0.29	8718	274687	38822	45.8	4833	5568	6068	370200
43	28/03	Middle Britata Spring	12.3	6.42	2.20	1598	42.5	271	0.26	5185	168094	26724	153.0	4639	3486	2061	432600
44	31/03	Kesel'ta Spring	12.3	7.07	12.91	8296	993	2860	<0.1	54817	4212603	219870	11.2	5990	1423	24416	149729
47	229/02	Kuan narzan, main ven	11	6.36	8.6	2227	3369	9384	<0.1	75155	1960547	49314	48	4761	15285	112975	162262

Table 2. (Contd.)

No. in Fig. 1	Sample no.	Mn, μg/l	Fe, μg/l	Co, μg/l	Ni, μg/l	Zn, μg/l	Ge, μg/l	Br, μg/l	Rb, μg/l	Sr, μg/l	Y, μg/l	Zr, μg/l	Cs, μg/l	Ba, μg/l	Th, μg/l	U, μg/l
1	8/01	776	5366	1.0	2.0	10.7	0.6	387	66.3	1664	1.4	1.7	67.7	48	0.12	2.3
1	8-4/01	549	236	0.76	3.1	3.0	0.6	353	65.2	1538	0.32	0.89	66.9	39	<0.07	2.2
2	9/01	1673	6806	1.0	5.0	7.8	32.5	3087	983.8	2754	4.4	24.2	1792	34.8	<0.07	7.5
26	10/01	1194	15230	0.68	2.5	14.2	14.7	577	525	1219	1.5	0.50	1783	16.6	0.12	0.20
5	24/00	1331	23930	13.0	23.9	35.6	37012	190	7.7	249	2.2	<0.05	0.82	42.4	<0.07	0.026
7	14/01	1727	2082	0.65	5.3	3	0.6	37.0	1.2	3327	3.6	2.3	0.1	13.5	0.11	0.35
7	14-15/01	1396	233	0.74	2.0	3	0.6	37.0	1.0	3340	0.2	1.5	0.1	11.7	0.19	0.52
11	K-4/00	2549	19020	5.8	10.9	14.2	<0.06	42.4	1.8	625	0.9	1.4	0.4	131	<0.07	1.6
14	K-7/00	5940	17471	13.1	23.1	10.8	<0.06	65.9	1.5	774	2.2	<0.05	0.18	206	<0.07	0.46
15	4/98	224	9597	0.62	3.6	17.1	12.7	427	278	1173	0.33	<0.05	136	443	<0.07	0.08
16	7/98	780	21290	0.45	7.6	21.6	35.4	370	230	1037	1.9	9.7	94.5	2161	<0.07	1.6
17	22/01	871	24341	1.9	5.5	9.5	4.6	813	28.1	1132	32.9	224	0.46	45.9	0.16	2.4
19	20/00	1164	6323	6.69	19.4	44.2	5.1	3831	145	<1	1.5	152	366	151	<0.07	0.14
28	29-2/01	538	8389	0.87	7.4	7.1	4.6	461	14.5	446	3.5	2.0	44.7	40.6	0.078	0.23
28	29-1/01	563	6211	1.2	7.4	5.8	23.5	2031	45.1	1013	1.5	7.5	115	90.3	<0.07	0.085
29	23/99	474	15055	0.28	3.7	<1	21.1	2167	366	4979	3.9	0.86	512	3282	0.029	0.073
33	8/03	191	1105	0.78	<1	<1	0.91	<44	4.9	1637	0.65	0.10	8.6	118	<0.006	0.060
34	9/03	388	7391	1.6	<1	<1	<0.06	<44	9.3	3726	0.26	0.049	10.2	303	<0.006	<0.003
35	10/03	120	175	0.85	<3	4.9	<0.1	129	28.4	3252	0.076	<0.05	14.5	205	<0.01	0.091
36	13/03	164	1529	1.8	2.2	<1	<0.06	<44	2.3	1786	0.49	0.12	1.0	162	<0.006	0.039
37	4/03	612	207	3.0	5.8	4.8	9.5	5353	1326	9358	0.44	<0.1	1438	381	<0.02	0.077
39	18/03	51.9	<8	1.7	3.4	<1	4.2	736	24.2	2833	0.91	0.34	25.6	291	<0.01	0.093
40	19/03	127	849	2.5	3.4	18.4	0.8	99.0	6.3	3137	1.5	0.20	9.1	86.9	<0.006	0.39
41	26/03	478	2400	1.2	1.6	1.9	1.0	57.2	5.2	1937	0.98	0.10	8.3	243	<0.006	0.51
42	27/03	252	2995	0.85	<1	1.3	2.1	151	13.7	2106	2.3	0.21	41.4	212	0.011	0.15
43	28/03	486	292	2.1	2.0	1.9	0.6	83.2	5.2	2308	0.79	0.10	8.9	491	<0.006	0.17
44	31/03	<0.3	733	0.25	3.7	4.8	0.81	1007	36.7	5215	0.052	2.5	52.5	1894	<0.01	<0.005
47	229/02	1676	3036	1.23	14	15	62	5971	489	5747	0.33	0.7	759	522	0.1	0.092

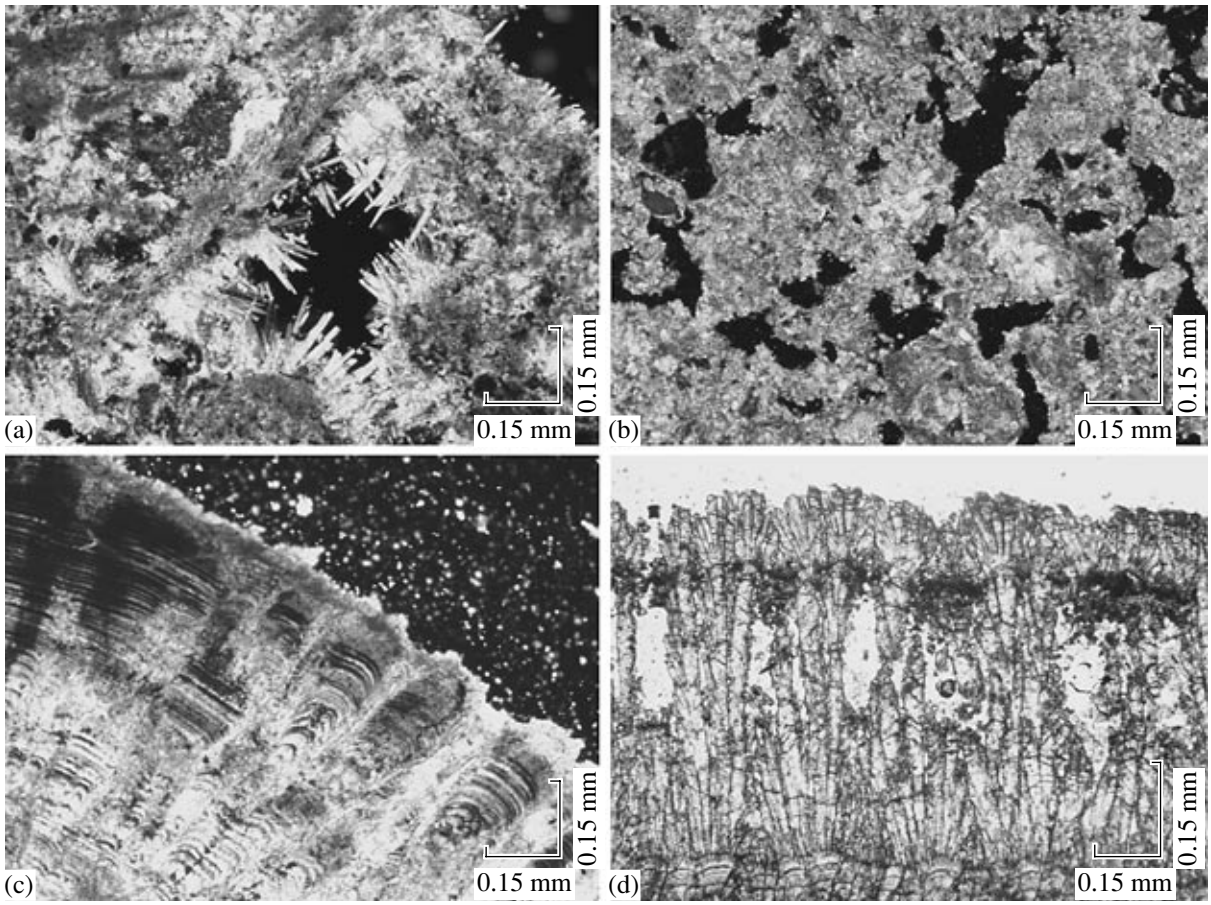

Fig. 3. Photomicrographs of carbonate travertines. (a) Spicular crystals of aragonite (zone B); (b) micritic crystals of calcite (zone B); (c) zonal travertines (zone C); (d) macrocrystalline zonal travertines (zone D).

of blue-green algae are widespread near the spring. Their filaments are covered by a loose layer of iron hydroxides.

Zone of ferrugination and incipient travertine formation (B) is traced from the lower boundary of zone A over a distance of 10–15 m (approximately 15–30 m from the spring). In this zone, carbonate sediments start to form in the mineral water stream, and the rate of iron hydroxide precipitation decreases. Sediments of this zone are most frequently porous and loose (more rarely, sediments of medium compactness).

Calcium carbonates precipitate in this zone in all places. They are represented by microcrystalline, frequently micrite calcite (Fig. 3b). In numerous pores, probably left after algae films, interlayers and nests of spicular aragonite crystals are encountered. The dark-brown color of carbonates is related to iron hydroxides. Ferruginous sediments sometimes make up separate interlayers. The thickness of carbonate-ferruginous deposits on the stream bottom reaches a few centimeters and increases toward the lower boundary of the zone.

Thus, zone B is transitional between the mass precipitation zone of iron hydroxides (A) to the zone of intense travertine formation (C).

Zone of intense travertine formation (C). This zone is characterized by the largest volume of travertine accumulation. Here, the travertines attain the maximum thickness (from a few to several tens of meters) and form the central part of the travertine dome. This zone is approximately 150 m long in the Upper Tokhana dome, and the maximum thickness of travertine accumulations can reach a few tens of meters.

In contrast to zones A and B, mineral water in Zone C spills in the form of a wide front on the dome surface, because the stream of mineral water is constantly blocked due to the intense settling of carbonates.

Here, carbonate sediments are bright and almost white (sometimes, slightly turned by iron hydroxides to yellow-orange, cream, or pink tints). The travertines are massive, hard, and distinctly zonal (Fig. 3c). Their surface is irregular and decorated with traces of the wave ripple type. The travertines are made up of elongate ingrowths of large calcite crystals separated by interlayers of fine-crystalline calcite. The alternation of such interlayers forms the zonation (layering) typical of travertines. Large calcite crystals have show wavy extinction. In cavities between crystals, one can see mineral-

ized filaments of blue-green algae and diatom shells. Aragonite is absent in this zone.

Zone of retarded travertine formation (D) is located at the base of the travertine dome. This zone corresponds to the final stage of precipitation of calcium carbonate from water. On the Upper Tokhana dome, its boundary is recorded by the perceptible thinning of travertines to several meters. By this moment, the water is completely free of carbonate excess. Therefore, travertines are accumulated very slowly.

Compact zonal travertines are formed in zone D. The surface of dry travertines has yellow-orange color owing to iron hydroxides. Algae in the stream give them a green color. They differ from travertines of zone C by a higher rate of calcite crystallization: the crystals are larger and elongate, like in Zone C (Fig. 3d). Fragments and outcrops of old weathered travertine accumulations are frequently found at the foot of travertine dome. Aragonite is absent in this zone as well.

Analogous zonation can also be traced in other springs. However, sometimes the zonation is not completely manifested. This depends on many factors, such as the degree of water saturation with calcium carbonate, concentration of CO_2 in water, temperature of water and ambient media, velocity of water flow, and others. If water has small concentrations of calcium (<250 mg/l), massive travertines (zones C and D) are not formed. For instance, the Upper Baksan (no. 26) and Uchkulanichi (no. 17) springs incorporate only thin algal–carbonate, intensely ferruginated crusts that cement terrigenous material on the stream bottom. In this case, one can talk only about incipient stages of travertine formation corresponding to zones A and B.

In thermal springs, such as the Proval Spring in Pyatigorsk (no. 27) and springs of the Verkhne-Karmadon area (no. 38), the travertine domes have a slightly different zonation. Because of high temperature, travertines begin to settle in them immediately, i.e., at outlets of mineral waters. Here, the zone of large-scale precipitation of iron hydroxides (A) coincides with the zone of massive travertines (C). Carbonates formed near the outlets of hot waters are often poorly crystallized and frequently characterized by the micritic structure. Layering in the travertines is less expressed and is documented only in lower parts of the travertine dome.

In general, the mineralogical investigations show that the bulk volume of the travertine dome is composed of calcite. Calcite crystals become larger toward the base of the dome. Aragonite precipitates sporadically and only near the spring, i.e., near the upper boundary of travertine formation (zones A and B). There is an impression that its crystallization postdates the travertine formation, because aragonite crystals are confined to pores in travertines and are absent on their surface.

GEOCHEMICAL ZONATION OF TRAVERTINE DOMES

We investigated spatial variations of chemical elements in the travertine domes at the following springs: Upper Tokhana, Irik-narzan, and Lashtrak (Tables 3 and 4, nos. 7, 1, and 28). Here, we took travertine samples for chemical analysis at different distances from the outlet of mineral water.

Morphological zonation of the travertine dome is naturally reflected in the chemical composition of travertines. First of all, this concerns the relationship between iron hydroxides and calcium carbonates. Generally, precipitation of iron compounds from solutions starts (and finishes) earlier than that of carbonates. Therefore, the Fe content in travertines is an order of magnitude lower toward the base of the dome. This is accompanied by the simultaneous decrease in concentrations of many other elements. The majority of these elements (Mn, Ni, As, Zn, Cu, Cr, V, Sc, K, P, Si, Al, REE, Th, U, Cs, Zr, Y, Be, and Ba) precipitate together with iron hydroxides. Rates of their precipitation in sediments are different. For example, Th is removed from water more rapidly than U. Hence, despite the general trend of decrease of concentrations of these elements along the dome strike (i.e., away from the spring), the U/Th ratio does not remain constant and increases five to seven times near the base of the dome. The Sr/Ba ratio also changes in a similar way. For the same reason, the Fe/Mn ratio can be almost 10 times lower toward the base of the dome. Such a high variability of chemical composition and some geochemical coefficients makes them unfit for reconstruction of the initial fluid composition.

In contrast to Fe, Mn, Th, U, and Ba, concentrations of REE change synchronously (Table 4, nos. 1, 7, and 28). Therefore, Y/Ho, Yb/Ho, Sm/Ru, and other ratios virtually do not change along the strike of the travertine dome. Correspondingly, the REE spectra do not change either (Fig. 4).

Concentrations of Na, Li, Mg, Sr, and S show a more conservative pattern. They remain almost stable or even increase (Sr and S) toward the base of the dome (Table 3, nos. 1, 7, and 28). Correspondingly, ratios of their concentrations in different parts of the travertine dome remain practically constant. Therefore, only these elements can be used for the reconstruction of specific features of salt composition in initial waters.

INTERRELATION OF CHEMICAL COMPOSITIONS OF CARBONATES AND WATERS

The aim of reconstruction of paleofluid regime is the determination of physicochemical characteristics of fluid: TDS content, predominant components of salt composition, redox conditions, temperature conditions of mineral precipitation, and base temperatures of water formation. We understand the “base” or “stratal”

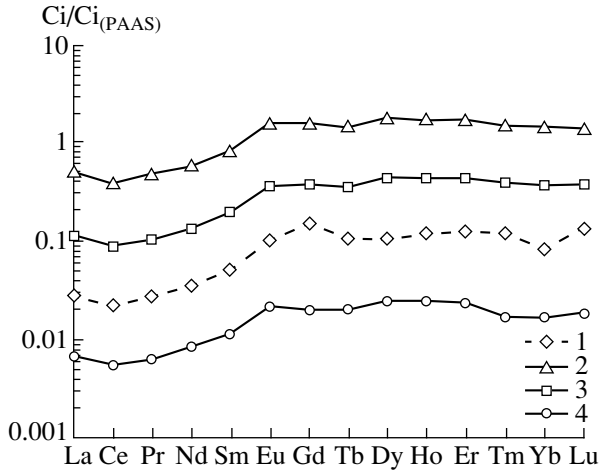

Fig. 4. PAAS-normalized REE spectra of (1) water and (2–4) travertines from the Upper Tokhana Spring. Travertines were taken at different distances from the spring: (2) 25 m (Sample T-3/01, zone B); (3) 50 m (Sample T-4/01, zone C); (4) 250 m (Sample T-6/01, zone D).

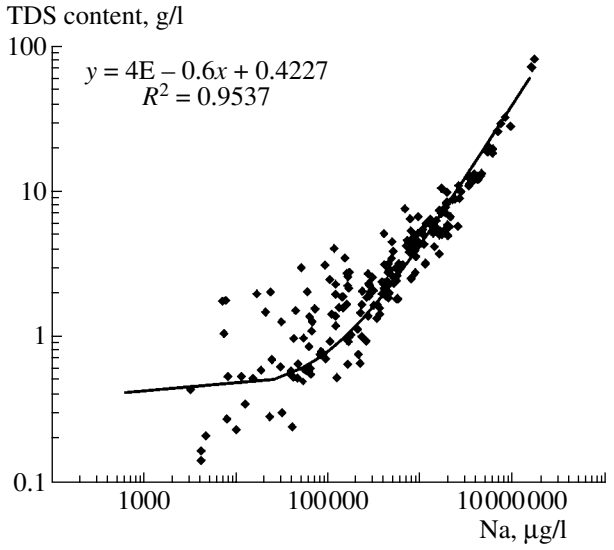

Fig. 5. Relationship between Na and Cl concentrations in mineral waters of the Caucasus region.

temperature as the formation temperature of salt composition in watermass (at maximal depths of water circulation). This temperature depends on the water circulation depth and local geothermal conditions. Correspondingly, the base temperature is always higher than water temperature in the spring. Therefore, the base temperature is not equivalent to the temperature of travertine formation. To resolve the problems formulated above, we have several approaches, e.g., the analysis of fluid inclusions in secondary minerals, study of the paragenesis of authigenic minerals and their chemical composition, and others.

Disler and Konovalova (1989) attempted to reconstruct specific features of the chemical composition of mineral waters based on the composition of travertines at springs of the Pamir. In particular, they proposed to use the silica concentration and Fe/Mn ratio for the reconstruction of temperature and redox conditions of fluids. However, these works were not continued because of a limited number of determined components.

Having results of the polycomponent chemical analysis of travertines and waters (Tables 2 and 3) at our disposal, we obtained the possibility to analyze a wider spectrum of chemical elements.

Since the Cl concentration in carbonates was not determined, TDS content of waters can be inferred from the concentration of alkaline metals that are present as admixture. Sodium is most suitable for this purpose. In the salt composition of waters, Na often represents the dominating cation. Therefore, knowing its concentration in water, one can also roughly estimate the TDS content in the solution (Fig. 5).

Comparison of Na concentrations in water (Table 2) and travertines (Table 3) shows that this problem can be resolved (Fig. 6a). Hence, using the regression equation cited in the figure, it is possible to calculate Na concentration in the solution and, finally, to obtain an idea about the degree of water mineralization (Fig. 5).

It should be noted that the most precise Na-based appraisal of mineralization can be made only for waters with the TDS content of more than 10 g/l (Fig. 5). If the TDS content is lower (especially, less than 2 g/l), scatter of data points increases and, consequently, the precision of TDS content determination diminishes. It is evident that the role of ions (Ca^{2+}, Mg^{2+}, HCO_3^-, and SO_4^{2-}) having larger molecular mass than Na^+ and Cl^- increases in weakly mineralized waters.

Thus, small changes in water mineralization (up to 100*n* mg/l) cannot be recorded by this method. It is evident that this method can only be used to distinguish carbonates formed from more contrast mineralized waters, i.e., with low (<2–3 g/l), intermediate (3–20 g/l), or high (more than 20 g/l) content of salts.

In addition to Na, Li can also be used for the determination of TDS content. Analogous correlations in the carbonate–water system are established for this element (Fig. 6b). However, results of the determination of water mineralization by this method seem to be less reliable.

Investigations of microcomponents in travertines make it also possible to get some ideas about the composition of host rocks. In this respect, Be is the most informative element. According to (Krainov *et al.,* 1966), CO_2-rich waters formed in crystalline rocks (granite gneisses) are characterized by a high Be concentration. The Be concentration in them sharply decreases when they contact with sedimentary rocks due to sorption on clay minerals.

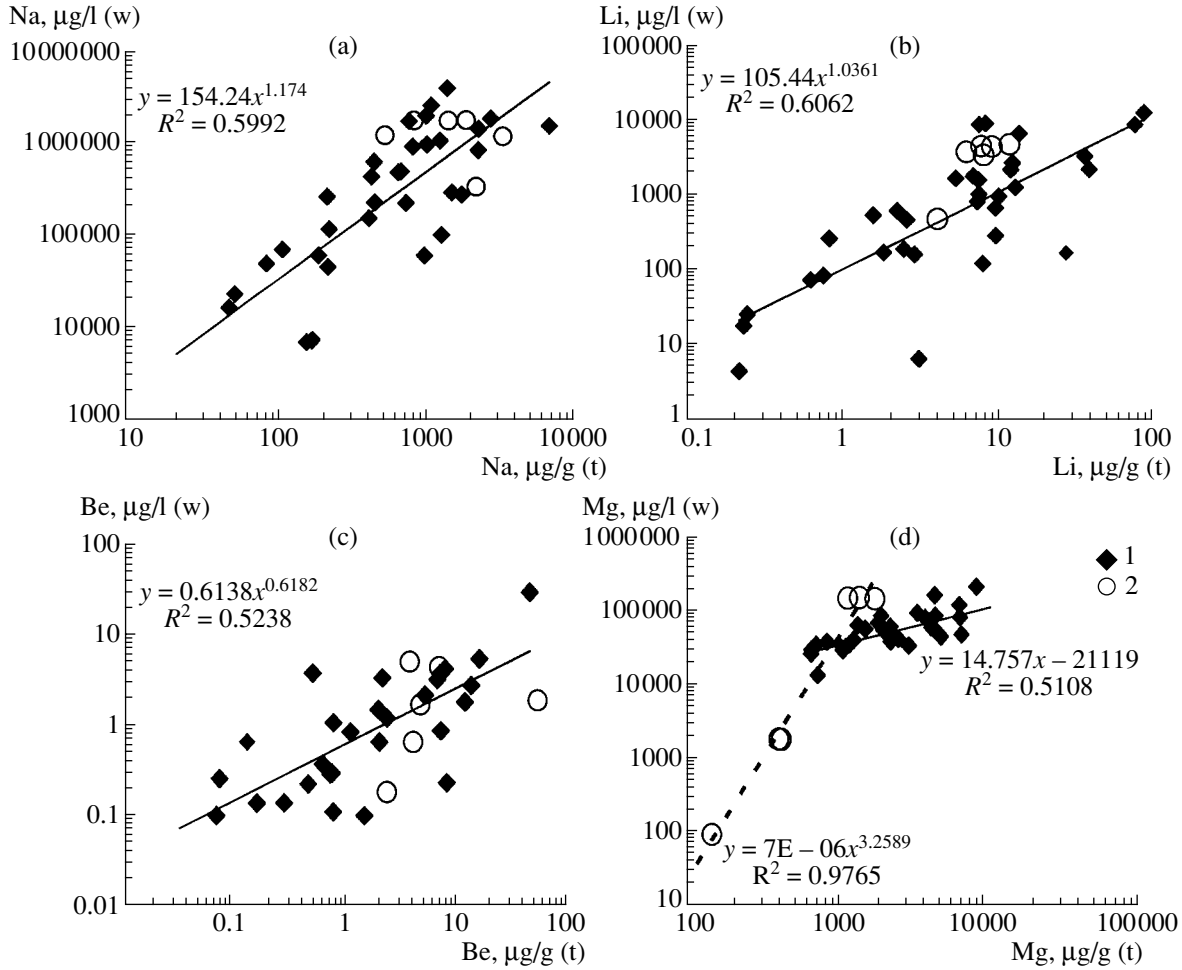

Fig. 6. Comparison of concentrations of (a) Na, (b) Li, (c) Be, and (d) Mg in travertine (t) and water (w). (1) Cold CO_2-rich waters of the Caucasus; (2) thermal N_2- and CO_2-rich waters of eastern Chukotka.

In mineral waters of the Greater Caucasus, maximal Be concentrations (1 to 5–30 μg/l) occur in CO_2-rich waters of the Main Ridge confined to crystalline massifs of Lower Paleozoic granite gneisses. In CO_2-rich waters of the Front Ridge and southern slope of the Greater Caucasus confined to Early–Middle Jurassic sedimentary complexes, the Be concentration sharply decreases to 0.05–0.5 μg/l. At foothills of the eastern and western Caucasus, Ciscaucasia, and Transcaucasia, N_2-rich and methane waters formed in weakly lithified Mesozoic–Cenozoic are distinguished by even lower Be concentrations (<0.05 μg/l). Hence, the correlation of Be concentrations in carbonates and waters can give an insight into the parental reservoir rocks.

Beryllium concentrations in the water–carbonate system have a ratio of approximately 1 : 1 (Fig. 6c). The Be concentration in the initial solution can be easily established on the basis of these estimations.

Analysis of the travertine–water system also allows the reconstruction of concentrations of other bivalent cations (Mg, Sr, and Ba) in the solution (Figs. 6d, 7a, and 7b). Similarly, one can appraise the sulfur concentration in water correlated with the concentration in travertine as approximately 1 : 10 (Fig. 7c). In mineral waters of the Greater Caucasus, sulfur in water is represented almost completely by sulfate ion (H_2S is absent or its concentration is negligible). Therefore, these calculations provide ideas about the concentration of SO_4^{2-} ion in fluid.

Spectra of REE, which are present in water and travertines, are generally similar (Fig. 4). Like in CO_2-rich waters, the majority of travertine samples demonstrate a relative increase of normalized concentrations from Sm–Eu to Lu. Moreover, the maximum normalized concentration is found in travertines in the Eu-enriched regions, such as the Sba and Sunna springs of southern Ossetia (nos. 39 and 40, respectively). Correspondingly, one can use chemogenic carbonates for the reconstruction of REE distribution in initial solutions. It is evident that the REE distribution in waters can also be investigated on the basis of chemical compositions of iron hydroxides that accumulate in springs more fre-

quently than travertines. However, this problem is outside the framework of our investigations. The issue of utilization of chemogenic carbonates for paleoreconstruction is also topical for mineral waters, because REE concentrations in them are frequently lower than the limit of detection by the ICP-MS method.

Thus, studying chemical composition of travertines, one can assess some specific features of salt composition of the initial fluid (Na, Li, Mg, S, Sr, Ba concentrations and TDS content) and the type of host rocks (based on the Be content).

Comparison of cold springs of the Caucasus and thermal waters of Chukotka (Figs. 6 and 7) shows that thermal and regional features of mineral waters generally do not affect the pattern of redistribution of chemical elements in the carbonate–water system. Magnesium is probably the sole exclusion (Fig. 6d). High-temperature (50–95°C) N_2- and CO_2-rich waters are especially prominent in the common group of data points. They are characterized by ultralow Mg concentrations (<10 mg/l). In contrast, warm (~20°C) CO_2-rich waters of Chukotka and their sediments are similar to springs and travertines of the Caucasus in terms of Mg concentrations. In this case, not only temperature conditions of carbonate precipitation, but also regional features of salt composition in waters can play a significant role.

POSSIBILITY OF THE USE OF TRAVERTINES FOR THE RECONSTRUCTION OF THE BASE TEMPERATURE OF FLUID GENERATION

Silica concentrations, as well as Li/Na, Li/Mg, and Na/K ratios in water solutions depend on temperature conditions of interaction in the water–rock system. Therefore, they are traditionally used as geothermometers for the determination of base temperatures of fluid generation of ground waters (Fournier and Truesdell, 1973; Fournier and Potter, 1979; Kharaka and Marner, 1989; Fouillac and Michard, 1981; and others). These geothermometers record the maximum temperature, at which fluid was formed in deep horizons of Earth's crust.

We have already discussed the problem of the choice of preferable geothermometer in our previous works devoted to the estimation of temperatures of fluid generation in mineral springs in the Elbrus and Kel'sk-Kazbek areas of the Greater Caucasus (Lavrushin and Polyak, 2001; Lavrushin and Makovozov, 2004). It was shown that the Na–Li geothermometer is more suitable for CO_2-rich waters of mountain regions, because the Si and Mg–Li temperatures can be distorted, e.g., due to the dilution of mineral waters with atmospheric precipitation. For more mineralized waters of sedimentary basins (>15 g/l), the Mg–Li geothermometer is more suitable for use (Lavrushin *et al.,* 2003b).

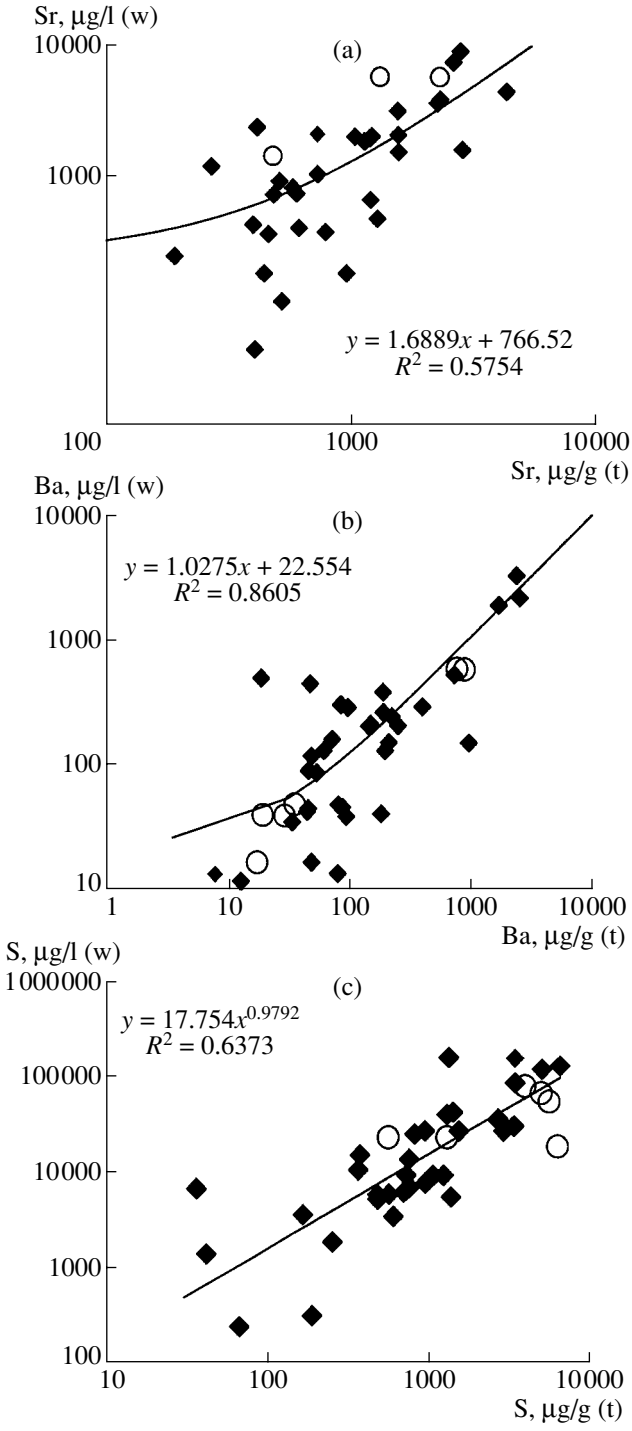

Fig. 7. Comparison of concentrations of (a) Sr, (b) Ba, and (c) S in travertine (t) and water (w). See Fig. 6 for legend.

We attempted to estimate the possibility of calculation of base temperatures of fluid generation from the data on chemical compositions of travertines.

Correlations for the water–carbonate system can be established almost for all chemical elements (Fig. 6) or their ratios (Figs. 8a–8c) involved in the calculations. This allows us to estimate concentrations of Li, Na,

Table 3. Chemical composition of carbonate travertines in the Greater Caucasus (concentrations are given in μg/l)

No. in Fig. 1	Sample no.	Location of sampling	Insoluble residue, %	Li	Be	B	Na	Mg	Al	Si	P	S	K	Ca
		Detection limit (DL)		0.08	0.04	2	3	4	3	5	12	16	74	110
		Elbrus area												
1	18/99	Irik-narzan Spring	10	9.6	2.2	7.4	409	4525	33.3	117	<DL	968	<DL	363718
1	8-1/01	Irik-narzan Spring, fresh travertine, beginning of stream	15.0	7.5	13.9	17.5	448	4446	542	182	66.3	1321	266	417156
1	8-4/01	Irik-narzan Spring, fresh travertine, lower part of dome (12 m downslope of spring)	15.7	10.1	8.3	29.0	728	3811	143	876	9.5	2751	205	467449
2	9-2	Upper Baksan Settlement, 2.5 m downslope of the spring, fresh compact porous ferruginated travertine	15.6	83.2	12.2	625	2965	4667	560	1445	87.5	3230	558	376814
2	9-1	Upper Baksan Settlement, travertine, 5 m downslope of spring vent	16.1	88.6	6.8	273	2255	3379	273	524	23.7	3515	311	427990
26	10/01	Upper Baksan Settlement, fresh travertine	49.2	36.7	0.79	218	1485	6438	3231	906	443	1367	1129	223129
5	24-1/00	Middle Shaukol Spring	18.8	7.9	0.78	<DL	216	<DL	3472	873	93.0	487	472	280822
7	14/98	Upper Tokhana Spring	0	<DL	<DL	<DL	170	1044	9.0	26.6	<DL	3493	<DL	352939
7	14a/98	Upper Tokhana Spring	0	0.27	0.14	<DL	113	1231	60.4	63.8	13.8	4143	<DL	362940
7	T-3	Upper Tokhana Spring, 25 m away from spring	12.0	3.1	1.5	<DL	154	2960	1802	1814	65.7	5143	193	401617
7	T-4	Upper Tokhana Spring, 50 m away from spring	8.6	0.27	0.40	<DL	141	726	104	563	26.1	6324	122	412421
7	T-6	Upper Tokhana Spring, 250 m away from spring	9.8	0.22	0.068	<DL	167	1195	43.2	62.4	9.9	6651	84.7	468035
8	18/98	Kizilkol River, ancient travertine	0	27.6	0.13	27.0	968	4846	41.1	126	<DL	1260	<DL	360556
9	K-1/00	Kizilkol River, ancient travertine	0	0.29	<DL	<DL	74.8	2028	129	172	18.1	45.0	<DL	342683
9a	K-2/00	Kizilkol River, ancient travertine	2	3.6	<DL	<DL	85.4	2924	2183	682	21.4	102	180	344599
10	K-3/00	Kizilkol River, ancient travertine	0	0.48	<DL	<DL	51.9	2603	70.6	58.6	<DL	72.3	<DL	361178
11	K4/00	Kizilkol River, carbonate sinters in well	7.4	1.8	2.0	<DL	187	2211	1030	3108	56.8	740	196	289554
12	K5-1/00	Kizilkol River, ancient travertine	0	0.24	<DL	<DL	73.8	2813	153	149	<DL	30.0	<DL	362059
12	K5-2/00	Kizilkol River, ancient travertine	1.2	1.7	<DL	<DL	20.0	2726	1211	534	<DL	46.0	<DL	343511
13	K6/00	Kizilkol River, ancient travertine	0	0.29	<DL	<DL	64.5	1973	103	96	18.1	99.3	<DL	362266
14	K7/00	Kizilkol River, fresh travertine	1.3	0.23	0.76	<DL	45.8	672	60.5	6164	<DL	255	<DL	305475
15	4/98-00	Biitiktebe River, cementation of sandy sediments in spring area	95	6.9	0.51	6.0	426	1524	2420	497	567	36.1	1273	4072
16	7/98	Biitiktebe River, fresh travertine	7.0	12.1	16.4	46.3	646	4196	639	3763	127	66.3	259	285162
17	22/01	Uchkulanichi River, fresh travertine	10	7.4	47.5	36.1	677	4407	4060	5588	49.7	835	181	131596
18	17/01	Amankol River, ancient aragonite	0	1.8	<DL	0.94	200	568	89.9	96.1	10.9	399	17.5	185151
19	20/00	Lower Ingushli Spring, fresh travertine	7.5	39.2	5.3	165	6871	1364	665	325	95.5	371	392	304699
21	148-4	Mt. Elbrus, upper reaches of the Ullu-kama River, dense well-crystallized slightly ferruginated travertine (fragment)	3.1	2.4	0.14	<DL	200	2551	1217	251	107	123	230	337245
27	Pr/00	Proval Spring, fresh travertine	2.2	4.3	5.8	<DL	780	2272	245	404	96.6	5399	156	341025

Table 3. (Contd.)

No. in Fig. 1	Sample no.	Location of sampling	Insoluble residue, %	Li	Be	B	Na	Mg	Al	Si	P	S	K	Ca
		Western Caucasus												
28	29-2/01	Lashtrak Spring (upper part of dome)	0	2.9	1.8	101	1735	739	294	8143	245	575	71.2	145795
28	29-5/01	Lashtrak Spring (base of dome)	0	2.6	0.17	30.3	1012	1085	105	1062	20.5	710	56.4	170647
		Northern Ossetia												
29	23/99	Kubus Spring, fresh travertine	0.7	13.8	8.1	297	812	1861	72.9	2484	23.9	167	119	351125
30	33/00	Khasiev Spring, fresh travertine	10.4	5.4	2.0	<DL	1080	2237	689	340	100	1443	120	311112
31	33-1/00	Tsmiakom-don River, cementation of gruss	47.6	19.9	0.47	<DL	67.3	4027	7476	654	387	197	314	173048
32	35/00	Well Tib 1, fresh sinters	0	7.5	7.2	22.3	2263	1948	848	218	40.5	1571	93.1	343977
33	8/03	Chel'diev narzan, old travertine	9.2	0.63	0.28	2.2	106	1132	46.1	55.0	30.3	487	140	489968
34	9/03	Karta Spring, fresh travertine	8.8	0.75	1.1	<DL	82.9	722	98.6	245	104	189	190	470736
35	10/03	Lower Zgil Spring, fresh carbonate crusts	9.3	1.6	0.12	2.7	445	2018	172	244	16.2	971	175	475062
36	13/03	Bubu Spring, fresh travertine	9.1	0.25	0.16	<DL	50.3	1281	83.6	136	28.6	779	117	424872
37	38-1/00	Upper Karmadon springs, upper part of dome	1.2	7.6	12.2	3.3	765	2244	128	1693	270	2745	216	339679
37	38-2/00	Upper Karmadon springs, lower part of dome	0.5	19.0	4.1	152	2107	1296	198	430	43.0	2908	399	338954
37	4/03	Upper Karmadon springs, fresh sinter of travertine after mudflow passage	10.6	8.4	7.4	46.2	999	2530	831	1298	103	3445	412	419091
38	Nar	Nar-don River, fragment of ancient travertine	2.2	4.3	0.18	18.4	799	3855	478	190	65.9	1269	208	365791
		Southern Ossetia												
39	18/03	Sba Spring, sinters of old travertine	12.5	13.0	2.4	19.6	1240	<DL	273	453	70.8	771	102	384873
40	19/03	Suna Spring (Sba-don River), fresh travertine	9.6	9.6	0.63	91.4	1263	6481	26.1	269	<DL	2963	193	428311
41	26/03	Britata Settlement, old travertine dome	12.8	2.5	0.46	<DL	220	1095	396	372	655	1082	268	438933
42	27/03	Upper Britata Spring, fresh travertine	11.7	2.2	0.74	<DL	214	852	398	522	37.4	1399	125	481985
42	27a/03	Upper Britata Spring, old travertine	17.1	2.1	0.51	<DL	64.2	1569	837	538	177	1117	238	446035
43	28/03	Middle Britata Spring, travertine from dry dome (flowed out before the earthquake)	12.1	0.83	0.073	<DL	<DL	667	288	208	54.2	614	324	493230
44	31/03	Kesel'ta Spring, carbonate veins from shales in area of mineral water venting	10.9	12.4	5.5	<DL	1387	8351	75.3	49.1	52.1	41.3	110	426911
		Eastern and Northeastern Caucasus (Dagestan)												
46	206/02	Berikei Settlement, Well 10, old travertines	2.9	21.0	0.11	82.0	3333	2729	1024	638	63.5	106	279	286148
47	229/02	Kuan narzan, left flank of Andiiskii Koisu	0.0	77.4	1.1	177.3	2743	6632	392	291	77.9	380	151	297620
49	D5/02	Quarry in Talgi Settlement, unaltered Upper Cretaceous limestones	25.7	6.0	0.17	<DL	195	3443	3066	881	756.7	286	603	214506
49	D6/02	Quarry, Talgi Settlement, large calcite crystals colored by bitumen, from fractures in Upper Cretaceous limestones	0.0	0.3	0.048	<DL	49.4	1281	119	39.0	14.3	42.1	40.8	311846
49	D13/02-1	Quarry, Talgi Settlement, small calcite crystals colored by bitumen, from fractures in Upper Cretaceous limestones	5.1	0.24	<DL	<DL	47.7	41805	134	57.6	<DL	258	45.3	213148
49	D7/02	Quarry, Talgi Settlement, aragonite vein in Upper Cretaceous limestones	0.0	2.2	0.031	<DL	151	2837	200	238	80.9	293	60.1	335764
		Taman Peninsula												
51	X/94	Fragment of carbonate vein from the Gorelyi mud volcano	19.3	2.5	0.15	6.9	148	2807	1324	799	57.7	97.3	527	408859

Table 3. (Contd.)

No. in Fig. 1	Sample no.	V	Cr	Mn	Fe	Co	Ni	Cu	Zn	Rb	Sr	Y	Zr	Mo	Sb	Cs	Ba	Pb	Th	U
Detection limit (DL)		0.2	2	0.2	16	0.06	2	0.1	3	0.01	0.6	0.02	0.03	0.03	0.01	0.008	0.4	0.3	0.01	0.005
Fore-Elbrus area																				
1	18/99	0.9	<DL	52.0	524	1.3	13.8	<DL	8.9	1.8	612	0.74	0.33	<DL	<DL	0.15	45.6	<DL	<DL	2.99
1	8-1/01	0.69	2.0	339	7434	1.4	4.5	1.0	64.1	2.3	597	4.9	0.22	0.30	0.031	2.2	80.7	1.4	0.17	0.78
1	8-4	<DL	1.8	2337	9855	2.6	4.3	<DL	36.0	0.91	1202	4.6	0.65	0.51	0.057	0.76	93.9	0.55	0.047	1.1
2	9-1	<DL	1.8	2475	6651	1.2	2.8	0.17	12.9	3.8	1572	4.6	3.6	0.47	0.050	10.4	33.6	0.76	0.059	2.4
2	9-2	0.25	5.6	2744	11270	1.3	4.5	0.33	20.7	6.4	1533	6.7	4.1	0.36	0.048	21.0	37.1	1.3	0.16	2.6
26	10-01	13.4	12.0	185	9159	2.8	7.7	3.7	25.4	12.4	1284	4.3	0.43	0.47	0.058	77.5	48.3	4.5	1.0	0.99
5	24-l/00	9.3	5.4	1064	14393	9.9	36.5	8.9	27.7	3.0	400	3.4	2.0	0.14	0.059	0.41	44.5	2.3	0.65	0.54
7	14/98	0.33	<DL	44.1	114	0.7	9.9	<DL	<DL	1.5	729	0.14	0.13	<DL	<DL	<DL	7.7	<DL	<DL	0.30
7	14a/98	1.1	<DL	2805	1638	1.7	14.5	<DL	<DL	2.8	1163	0.79	5.2	<DL	0.033	<DL	17.0	<DL	<DL	0.050
7	T-3	6.6	29.0	17790	54405	5.9	28.5	1.7	9.6	0.85	1037	71.3	5.1	0.93	0.239	0.35	79.5	0.68	0.058	0.38
7	T-4	0.28	1.5	5101	12302	1.1	1.0	<DL	3.3	0.35	1201	17.9	1.4	0.15	0.043	0.10	23.2	0.31	0.012	0.30
7	T-6	<DL	1.0	2361	866	1.1	0.39	0.69	3.6	0.39	1222	0.70	1.6	0.17	0.047	0.067	12.6	0.35	0.006	0.26
8	18/98	0.73	<DL	966	329	7.5	20.0	0.78	25.4	2.8	957	0.061	0.13	<DL	0.038	0.21	61.2	<DL	<DL	0.21
21	148-4	5.1	3.0	51.5	3023	1.5	10.2	2.2	60.0	2.7	92.8	32.7	0.21	0.041	<DL	7.7	28.6	4.9	2.0	2.6
9	K-1/00	1.4	<DL	16.1	272	0.63	10.9	3.9	8.2	0.080	83.6	9.0	0.76	<DL	0.029	0.038	15.6	0.84	0.062	0.10
9a	K-2/00	6.3	7.8	187	3029	2.5	10.2	11.1	11.1	0.46	145	1.2	0.19	<DL	0.024	0.49	60.4	1.6	0.11	0.068
10	K-3/00	1.3	<DL	4.7	161	0.48	5.3	0.66	<DL	0.016	150	1.0	<DL	<DL	<DL	0.021	6.4	0.59	<DL	0.19
11	K4/00	8.6	7.0	3873	40927	7.7	13.7	9.2	37.1	1.4	439	3.7	3.4	0.085	0.055	0.28	197	1.4	0.30	1.1
12	K5-1/00	0.88	<DL	12.6	248	0.66	15.9	58.5	6.4	0.024	87.0	0.77	1.1	<DL	<DL	0.020	3.5	0.36	<DL	0.31
12	K5-2/00	3.8	12.0	34.5	1494	1.7	20.9	3.0	6.1	0.08	98.9	0.15	0.27	<DL	<DL	0.064	28.4	0.53	<DL	0.025
13	K6/00	0.92	<DL	26.4	263	0.7	7.2	1.1	<DL	0.040	101	0.49	0.15	<DL	<DL	0.020	35.2	<DL	<DL	0.20
14	K7/00	5.2	<DL	4835	62641	13.3	15.3	<DL	25.6	0.047	189	17.7	1.8	0.082	0.049	<DL	252	<DL	0.016	0.25
15	4/98-00	16.0	12.0	57.6	6514	1.2	4.8	3.6	11.1	7.8	23.9	2.9	1.5	0.13	<DL	10.9	47.6	1.7	2.0	0.31
16	7/98	7.0	<DL	2905	28017	4.6	6.7	<DL	31.7	2.9	786	9.8	16.4	0.13	<DL	3.2	2511	0.81	2.0	0.66
17	22/01	28.8	8.2	1066.4	68307	4.6	7.5	42.1	20.3	1.6	396	86.0	338.0	20.2	0.4	0.26	86.8	4.2	3.7	3.7
18	17/01	1.7	1.3	12.7	446	0.63	0.89	0.39	1.5	0.12	345	0.14	0.20	<DL	<DL	0.019	12.0	0.17	0.037	6.5
19	20/00	5.2	<DL	419	10158	3.5	16.7	2.7	27.9	2.4	3578	3.9	10.5	<DL	0.15	4.2	958	1.4	0.31	0.14
27	Pr/00	1.4	<DL	169	606	1.0	8.6	1.4	10.0	0.98	2085	0.46	0.13	<DL	0.12	0.83	39.0	1.9	0.049	0.091

Table 3. (Contd.)

No.in Fig. 1	Sample no.	V	Cr	Mn	Fe	Co	Ni	Cu	Zn	Rb	Sr	Y	Zr	Mo	Sb	Cs	Ba	Pb	Th	U
Western Caucasus																				
28	29-2/01	15.6	1.8	400.6	50203	0.9	1.6	5.4	10.7	0.3	518	20.6	2.0	<DL	<DL	1.5	182	0.61	0.090	0.072
28	29-5/01	2.8	0.66	448.3	5689	0.95	0.94	0.71	2.4	0.25	457	1.8	1.1	<DL	<DL	0.70	46.0	0.33	0.023	0.037
Northern Ossetia																				
29	23/99	2.5	<DL	650	16199	2.4	14.7	0.76	53.0	0.8	2269	6.3	0.91	<DL	0.12	2.1	2378	0.54	0.094	0.026
30	33/00	4.0	4.5	1635	4809	1.8	10.9	5.5	10.7	0.82	1557	7.6	0.27	0.065	0.10	3.0	96.9	2.9	0.23	0.023
31	33-1/00	18.6	20.7	1234	27038	10.0	43.5	30.5	68.5	1.3	98.7	1.6	0.49	0.82	0.13	1.4	10.2	20.6	2.8	0.23
32	35/00	1.6	3.4	123	8336	1.1	13.3	<DL	<DL	3.4	1567	0.61	0.34	<DL	0.076	0.34	212	<DL	<DL	<DL
33	8/03	<DL	0.78	340	265	1.0	0.83	1.8	6.2	0.27	481	0.61	0.056	0.20	0.027	0.059	48.4	0.23	0.004	<DL
34	9/03	<DL	2.1	945	3281	1.7	2.0	0.83	4.2	0.37	413	0.24	0.044	0.23	0.029	0.20	85.0	0.25	0.0027	<DL
35	10/03	<DL	1.0	604	3359	1.7	0.37	0.62	12.0	0.56	1189	0.65	0.036	0.15	0.037	0.21	144.4	0.53	0.021	<DL
36	13/03	<DL	1.1	312	1807	1.1	1.6	0.57	2.6	0.26	576	1.4	0.14	0.14	0.059	0.045	72.1	0.43	0.0087	<DL
37	38-1/00	3.6	5.5	1885	24902	5.0	10.6	46.9	32.6	1.1	2641	18.8	3.6	0.060	0.33	1.9	191	34.6	0.035	0.39
37	38-2/00	2.6	10.3	2110	6874	5.3	10.0	6.5	14.5	2.0	2815	2.5	0.58	<DL	0.14	4.3	199	1.6	0.070	0.39
37	4/03	1.2	2.0	2912	17147	4.0	4.2	6.8	39.1	3.0	2815	10.4	0.10	0.14	0.185	5.5	190.2	4.6	0.23	0.10
38	Nar	2.5	3.3	91.1	956	1.7	14.4	10.9	31.8	0.37	728	0.56	0.085	<DL	0.047	0.33	61.5	1.7	0.016	0.11
Southern Ossetia																				
39	18/03	<DL	1.6	195	572	0.9	<DL	0.93	4.4	0.51	2860	2.9	0.065	0.32	0.044	0.55	399.6	0.60	0.041	<DL
40	19/03	<DL	1.2	281	368	1.1	2.2	0.93	5.1	0.31	1138	2.8	0.15	0.15	0.036	0.29	53.6	0.11	0.009	0.212
41	26/03	0.6	1.0	1550	2870	3.4	4.8	2.7	17.1	1.0	508	1.3	0.21	0.43	0.13	0.30	225	12.4	0.03	0.11
42	27/03	1.0	1.3	823	8790	1.7	1.1	0.69	8.7	0.47	728	10.1	0.13	0.25	0.042	0.64	150	0.68	0.069	0.066
42	27a/03	0.9	2.5	923	6167	3.8	14.0	7.4	18.3	1.5	231	8.9	0.21	0.53	0.14	0.31	17.2	1.8	0.14	0.20
43	28/03	<DL	1.2	21	656	1.0	2.2	0.88	4.3	1.0	267	3.3	0.042	0.33	0.046	0.64	18.7	0.66	0.019	0.079
44	31/03	<DL	<DL	312	30900	0.8	0.5	<DL	4.2	0.2	2324	0.3	4.1	0.08	0.045	0.051	1689	0.2	0.013	<DL
Eastern Caucasus (Dagestan)																				
46	206/02	5.5	2.3	226	6854	2.0	4.1	4.6	12.8	7.7	13621	1.2	0.36	0.22	0.064	1.1	10894	3.6	0.24	0.04
47	229/02	0.72	<DL	3508	1102	1.6	2.3	1.2	4.8	2.5	4324	0.41	0.051	<DL	0.036	3.7	731	0.55	0.055	<DL
49	D5/02	12.4	7.8	400	4917	24.2	48.2	4.2	162	8.6	507	25.8	0.090	0.39	0.025	0.6	15.1	7.8	1.6	0.16
49	D6/02	0.74	<DL	522	3119	0.59	0.75	<DL	2.7	0.18	650	3.4	0.31	<DL	0.048	<DL	16.8	0.72	0.0053	<DL
49	D13/02-1	<DL	<DL	451	26834	2.6	12.6	0.73	7.6	0.19	429	2.7	0.14	0.070	0.020	<DL	11.6	0.54	0.0073	<DL
49	D7/02	1.5	<DL	258	466	0.92	4.06	0.66	4.1	0.82	746	0.79	0.084	0.048	0.034	0.089	93.4	0.32	0.035	0.18
Taman Peninsula																				
51	X/94	4.4	8.1	5304	14070	2.7	4.7	3.1	14.0	2.6	580	12.2	0.11	0.48‘	0.019	0.30	30.8	2.1	0.47	0.16

Table 4. Concentrations of rare earth elements (μg/g) in travertines and vein carbonates of the Greater Caucasus

No. in Fig. 1	Sample no.	Location of sampling	La	Ce	Pr	Nd	Sm	Eu	Gd	Tb	Dy	Ho	Er	Tm	Yb	Lu	Hf
		Elbrus area															
1	18/99	Irik-narzan Spring	0.033	0.10	0.010	0.057	<0.008	0.020	0.030	0.006	0.041	0.012	0.038	0.011	0.065	0.012	<0.003
1	8-1/01	Irik-narzan Spring, fresh travertine, beginning of stream	1.2	2.6	0.32	1.4	0.32	0.086	0.42	0.065	0.44	0.12	0.29	0.036	0.25	0.032	<0.003
1	8-4/01	Irik-narzan Spring, fresh travertine, lower part of dome (12 m downslope of spring)	0.35	0.63	0.08	0.41	0.11	0.05	0.19	0.035	0.30	0.10	0.26	0.031	0.22	0.035	<0.003
2	9-2	Upper Baksan Settlement, lower narzan, 2.5 m downslope of spring, fresh travertine, compact porous ferruginated	0.6	1.2	0.15	0.68	0.16	0.07	0.27	0.05	0.45	0.13	0.50	0.072	0.59	0.098	<0.003
2	9-1	Upper Baksan Settlement, lower narzan, 5 m downslope of the vent, travertine	0.33	0.68	0.08	0.34	0.089	0.038	0.16	0.031	0.30	0.088	0.32	0.051	0.41	0.075	<0.003
26	10/01	Upper Baksan Settlement, fresh travertine	4.9	10.7	1.3	5.2	1.2	0.17	1.2	0.18	0.98	0.18	0.49	0.056	0.33	0.041	<0.003
5	24-l/00	Lower Shaukol Spring	1.7	3.8	0.54	2.2	0.46	0.13	0.76	0.088	0.58	0.12	0.31	0.045	0.30	0.038	0.021
7	14/98	Upper Tokhana Spring	0.04	0.08	0.012	0.09	0.012	<0.01	0.022	<0.003	0.044	0.007	0.014	<0.004	0.0087	0.0040	
7	14a/98	Upper Tokhana Spring	0.34	0.53	0.082	0.40	0.086	0.024	0.14	0.019	0.11	0.027	0.056	0.0060	0.037	0.0087	0.032
7	T-3	Upper Tokhana Spring, 25 m away from spring	19.0	30.1	4.1	18.2	4.5	1.7	7.2	1.1	7.6	1.68	4.9	0.58	3.9	0.59	<0.003
7	T-4	Upper Tokhana Spring, 50 m away from spring	4.2	6.9	0.89	4.1	1.1	0.39	1.7	0.27	1.9	0.42	1.2	0.15	1.0	0.16	<0.003
7	T-6	Upper Tokhana Spring, 250 m away from spring	0.26	0.43	0.06	0.27	0.063	0.023	0.093	0.015	0.11	0.024	0.067	0.0066	0.047	0.0078	<0.003
9	K-1/00	Kizilkol River, ancient travertine	0.61	0.31	0.24	1.3	0.27	0.10	0.56	0.082	0.70	0.21	0.63	0.091	0.65	0.12	0.014
9a	K-2/00	Kizilkol River, ancient travertine	0.45	1.0	0.16	0.71	0.17	0.052	0.24	0.040	0.25	0.065	0.12	0.018	0.11	0.018	0.0078
10	K-3/00	Kizilkol River, ancient travertine	0.13	0.10	0.038	0.22	0.062	<0.01	0.096	0.015	0.17	0.044	0.11	0.024	0.11	0.014	<0.003
11	K4/00	Kizilkol River, carbonate sinters in well	1.4	3.3	0.5	2.1	0.5	0.12	0.53	0.07	0.52	0.15	0.34	0.043	0.38	0.044	0.020
12	K5-1/00	Kizilkol River, ancient travertine	0.063	0.069	0.022	0.11	0.012	<0.01	0.056	0.007	0.087	0.029	0.074	0.009	0.089	0.015	0.022
12	K5-2/00	Kizilkol River, ancient travertine	0.059	0.16	0.020	0.13	0.030	<0.01	0.033	0.006	0.054	0.009	0.013	<0.004	0.0073	<0.002	<0.003
13	K6/00	Kizilkol River, ancient travertine	0.25	0.22	0.064	0.26	0.033	0.014	0.060	0.006	0.063	0.021	0.033	<0.004	0.045	0.0032	<0.003
14	K7/00	Kizilkol River, fresh travertine	3.1	4.3	0.64	2.6	0.47	0.19	0.90	0.13	0.96	0.33	0.74	0.10	0.74	0.10	<0.003
15	4/98-00	Biitiktebe River	7.0	17.6	2.6	9.5	1.7	0.15	1.4	0.17	0.91	0.17	0.37	0.050	0.28	0.037	0.036
16	7/98	Biitiktebe River	2.7	6.5	1.0	3.9	1.1		1.7	0.26	1.8	0.43	0.98	0.12	0.76	0.11	0.084
17	22/01	Uchkulanichi River	26.1	78.2	8.0	28.5	7.2	1.4	8.7	1.6	11.9	2.8	9.8	1.7	11.0	1.8	3.6
18	17/01	Amankol River, ancient aragonite	0.12	0.29	0.037	0.16	0.055	0.009	0.028	0.0038	0.031	0.003	0.01	0.0033	<0.004	<0.002	<0.003
19	20/00	Lower Ingushli Spring	0.83	2.1	0.29	1.2	0.30	<0.01	0.43	0.072	0.46	0.14	0.37	0.047	0.30	0.049	0.020
21	148-4	Ullu-kam River, fragment of travertine from terminal moraine	32.1	14.7	8.4	31.0	5.5	1.1	5.5	0.67	4.3	1.1	2.4	0.24	1.4	0.16	0.031
27	Pr/00	Pyatigorsk, Proval Spring	0.33	0.74	0.084	0.35	0.09	<0.01	0.10	0.017	0.12	0.023	0.058	0.01	0.049	0.004	0.013

Table 4. (Contd.)

No. in Fig. 1	Sample no.	Location of sampling	La	Ce	Pr	Nd	Sm	Eu	Gd	Tb	Dy	Ho	Er	Tm	Yb	Lu	Hf
		Western Caucasus															
28	29-2/01	Lashtrak Spring (upper part of dome)	4.9	9.0	1.3	5.9	1.7	0.50	2.2	0.35	2.5	0.52	1.5	0.21	1.3	0.18	0.03
28	29-5/01	Lashtrak Spring (dome base)	0.37	0.76	0.11	0.49	0.16	0.048	0.20	0.022	0.19	0.048	0.13	0.020	0.13	0.016	<0.003
		Northern Ossetia															
29	23/99	Kubus Spring	0.65	1.3	0.19	0.87	0.20	<0.01	0.42	0.062	0.52	0.17	0.50	0.077	0.52	0.10	0.016
30	33/00	Khasiev Spring		1.1	0.25	1.3	0.49	0.16	0.86	0.13	0.98	0.25	0.61	0.077	0.49	0.074	<0.003
31	33-1/00	Tsmiakom-don River	3.2	6.8	1.1	4.2	1.1	0.22	1.1	0.15	0.64	0.12	0.26	0.017	0.15	0.017	<0.003
32	35/00	Well Tib 1	0.024	0.063	0.0072	0.078	0.036	<0.01	0.045	0.0049	0.066	0.025	0.041	<0.004	0.013	0.0027	<0.003
33	8/03	Chel'diev Narzan, old travertine	<0.009	0.11	0.016	0.10	0.023	0.011	0.035	<0.003	<0.006	0.014	0.039	0.0036	0.035	0.005	<0.003
34	9/03	Karta Spring, fresh travertine	0.066	0.13	0.017	0.075	0.023	0.011	0.023	<0.003	<0.006	<0.003	0.020	0.0016	0.014	0.002	<0.003
35	10/03	Lower Zgil Spring, fresh carbonate crusts	0.16	0.29	0.049	0.26	0.076	0.036	0.092	0.015	0.10	0.022	0.048	0.0066	0.037	0.006	<0.003
36	13/03	Bubu Spring, fresh travertine	0.12	0.23	0.039	0.23	0.048	0.023	0.075	0.014	0.11	0.034	0.093	0.013	0.083	0.014	<0.003
37	38-1/00	Upper Karmadon springs, upper part of dome	3.3	4.8	0.84	3.2	0.9	0.34	1.62	0.29	2.32	0.67	1.75	0.221	1.35	0.171	0.016
37	38-2/00	Upper Karmadon springs, lower part of dome	0.36	0.70	0.12	0.42	0.077	0.033	0.17	0.028	0.21	0.065	0.16	0.022	0.15	0.025	<0.003
37	4/03	Upper Karmadon springs, fresh sinter of travertine after mudflow passage	1.2	2.5	0.30	1.2	0.30	0.10	0.44	0.076	0.68	0.19	0.70	0.10	0.62	0.085	<0.003
38	Nar	Nar-don River	0.16	0.33	0.056	0.27	0.084	0.025	0.12	0.021	0.12	0.023	0.044	0.0087	0.026	0.0046	<0.003
		Southern Ossetia															
39	18/03	Sba Spring, sinters of old travertine	0.69	1.1	0.18	0.83	0.22	0.093	0.29	0.043	0.30	0.069	0.21	0.027	0.18	0.029	<0.003
40	19/03	Suna (Sba-don) Spring, fresh travertine	0.081	0.33	0.064	0.30	0.074	0.030	0.11	0.023	0.16	0.047	0.16	0.030	0.16	0.029	<0.003
41	26/03	Britata Settlement, old travertine dome	0.35	0.59	0.10	0.43	0.12	0.055	0.16	0.023	0.15	0.035	0.094	0.013	0.085	0.014	<0.003
42	27/03	Upper Britata Spring, fresh travertine	1.8	2.7	0.44	2.1	0.6	0.20	0.79	0.12	0.90	0.21	0.68	0.10	0.69	0.11	<0.003
42	27a/03	Upper Britata Spring, old travertine	3.0	3.7	0.70	3.1	0.78	0.23	0.91	0.14	0.90	0.20	0.57	0.07	0.48	0.07	<0.003
43	28/03	Middle Britata Spring, travertine from dry dome	0.80	0.43	0.19	0.93	0.19	0.062	0.25	0.036	0.25	0.06	0.16	0.021	0.14	0.02	<0.003
44	31/03	Kesel'ta Spring, carbonate veins from shales in area of mineral water venting	0.061	0.10	0.020	0.11	0.053	0.14	0.050	0.0083	<0.006	<0.003	0.023	0.0036	0.025	0.004	<0.003
		Eastern Caucasus (Dagestan)															
46	206/02	Berikei Settlement, Well 10	1.1	2.0	0.24	1.1	0.31	<0.01	0.22	0.028	0.14	0.021	0.056	0.017	0.754	0.085	<0.003
47	229/02	Kuan narzan, left flank of Andiiskii Koisu	0.11	0.23	0.024	0.13	0.053	<0.01	0.062	0.011	0.047	0.0086	0.023	0.0034	0.050	0.008	<0.003
49	D5/02	Quarry, Talgi Settlement, unaltered Upper Cretaceous limestones	14.1	21.7	4.7	18.5	4.2	0.90	3.8	0.5	2.9	0.55	1.4	0.18	1.0	0.13	<0.003
49	D6/02	Quarry, Talgi Settlement, large crystals of calcite colored by bitumen, from fractures in Upper Cretaceous limestones	0.58	0.80	0.17	0.67	0.18	0.038	0.19	0.026	0.21	0.051	0.14	0.016	0.109	0.011	<0.003
49	D13/02-1	Quarry, Talgi Settlement, small calcite crystals colored by bitumen, from fractures in Upper Cretaceous limestones	0.55	0.82	0.14	0.63	0.13	0.033	0.18	0.027	0.18	0.029	0.10	0.007	0.059	0.009	<0.003
49	D7/02	Quarry, Talgi Settlement, aragonite vein in Upper Cretaceous limestones	0.30	0.35	0.05	0.29	0.059	0.031	0.061	0.0068	0.051	0.0087	0.043	0.0046	0.032	0.006	<0.003
		Taman Peninsula															
51	X/94	Fragment of carbonate vein from the Gorelyi mud volcano	9.7	20.3	2.2	8.8	1.9	0.50	2.0	0.33	2.0	0.37	0.93	0.10	0.56	0.071	<0.003

Mg, and Si in the initial solution based on chemical compositions of travertines. The values obtained can be used in already known formulas for the calculations of base temperatures with the help of hydrochemical geothermometers (Fournier and Truesdell, 1973; Fournier and Potter, 1979; Kharaka and Marner, 1989; Fouillac and Michard, 1981, and others). The Na–K geothermometer is the sole exclusion, because the reconstruction of K concentration in solution based on the chemical composition of travertine does not give satisfactory results.

The base temperature of water formation can also be appraised by comparing values of Li/Mg, Li/Na or Si in travertines with values of base temperatures calculated from the available chemical analyses of water (Table 2). Analytical expressions that connect the calculated water temperature and ratios (or concentrations) of elements in travertines are given in Figs. 8d–8f.

Comparison of chemical compositions of travertines with base temperatures calculated from chemical analyses of cold and thermal waters of the Greater Caucasus and Chukotka shows that regional peculiarities of water composition formation and temperature conditions of travertine formation almost do not affect the estimates based on Na–Li and Li–Mg geothermometers (Figs. 8d, 8e). According to the Si geothermometer, springs in these two regions appreciably differ, particularly, high-temperature springs of Chukotka (Mechigmen springs, up to 95°C) (Fig. 8f). Hence, estimations of base temperatures based on the Si geothermometer are least precise.

The base temperatures determined for different parts of travertine domes in cold springs (Upper Tokhana, Irik-narzan, and Lashtrak) showed that they change along the strike of the travertine dome. This is particularly evident on a large dome of the Upper Tokhana Spring. Here, Na–Li and Mg–Li temperatures decrease almost by a factor of two from the summit to bottom of the dome. At the same time, water samples taken from the stream at different distances from the spring are virtually similar with respect to base temperatures. It is evident that estimations of base temperatures from travertine analyses are affected by the carbonate precipitation rate. If the precipitation is intense, the carbonates contain more admixtures (including Li and Na).

However, this trend is less prominent on small domes extending over a few tens of meters (Irik-narzan, Upper Baksan, and Lashtrak), and readings of geothermometers in upper and lower parts of the dome at a distance of up to 20–30 m are almost similar (the discrepancy does not exceed 5–15°C).

Thus, data on the chemical composition of travertines allow us to estimate the base temperatures of fluid generation. The best results can be achieved during investigations of small domes, whose size does not exceed a few tens of meters. As linear size of the dome increases, the precision of such estimations diminishes.

PECULIARITIES OF ISOTOPIC COMPOSITION OF TRAVERTINES

The $\delta^{13}C$ and $\delta^{18}O$ values in travertines of the Greater Caucasus vary from –6.8 to + 16.3‰ (average + 5.8‰, n = 66) and from +16.4 to +28.1‰ (average +23.5‰, n = 66) respectively (Table 5). Thus, travertines are often appreciably heavier in terms of $\delta^{13}C$ than marine carbonates (~0‰). Isotopically heavy carbonates are often encountered in travertines from other mountain systems: the Alps, Andes, Kamchatka, and others (Gonfiantini *et al.,* 1968; Chafetz *et al.,* 1991; Valero-Garces *et al.,* 1999; Naboko *et al.,* 1999). Isotopically light (in terms of $\delta^{13}C$) carbonates formed from waters with methane gas constituent are sharply different.

Isotopic characteristics of travertines are dictated by many factors, for instance, by isotopic composition of the initial carbon dioxide, temperature conditions of carbonate precipitation, and the rate of oversaturation of waters with calcium carbonates.

In springs of the Main Ridge of the Greater Caucasus, $\delta^{13}C$ values in the spontaneous CO_2 change from –8 to –5‰ (Lavrushin *et al.,* 2001b). Virtually all carbonates are in disequilibrium with such carbon dioxide in terms of $\delta^{13}C$ values. Generally, difference between $\delta^{13}C$ values in $CaCO_3$ and CO_2 is 11–14‰, reaching in some cases 24‰ (Upper Tokhana Spring) (Table 5, no. 7).

Figure 9 shows that $\delta^{13}C$ and $\delta^{18}O$ values in carbonates are directly correlated both within the entire Caucasus region and in separate domes (Irik-narzan no. 1 and Lower narzan no. 2) in the Upper Baksan Settlement, Upper Tokhana no. 7, and Lashtrak no. 28). This can be explained by the mixing of fluids with different isotopic compositions of carbon and oxygen. The proposed hypothesis is valid for the explanation of changes in isotope characteristics of carbonates within the entire Caucasus region, i.e., it takes into consideration the regional variations in isotopic composition of the spontaneous CO_2 (Lavrushin *et al.,* 2001b, 2003a). However, this mechanism cannot be applied for the interpretation of $\delta^{13}C$ and $\delta^{18}O$ values in separate domes. In the last case, the mixing of fluids of different ages, which provoke intense variations in $\delta^{13}C$ (CO_2), is unlikely. In the Elbrus area, carbon isotopic composition in the spontaneous CO_2 is rather stable both in area (–8 to –5‰) and time. The range of variations $\delta^{13}C$ (CO_2) values during the controlled sampling period does not exceed 0.5–1.0‰.

Sampling of travertine domes along the strike showed that $\delta^{13}C$ and $\delta^{18}O$ values always change regularly: with increasing distance from the center of mineral water discharge, carbon and oxygen isotopic compositions of carbonates become heavier (Table 5, nos. 1, 2, 7, 27–29, and 37). This trend is most prominent in the Upper Tokhana Spring (Figs. 10a, 10b). Here, $\delta^{13}C$ and $\delta^{18}O$ values change from +3.8 to +16.3‰ and from +24.6 to +28.1‰, respectively, over a distance of approximately 350 m.

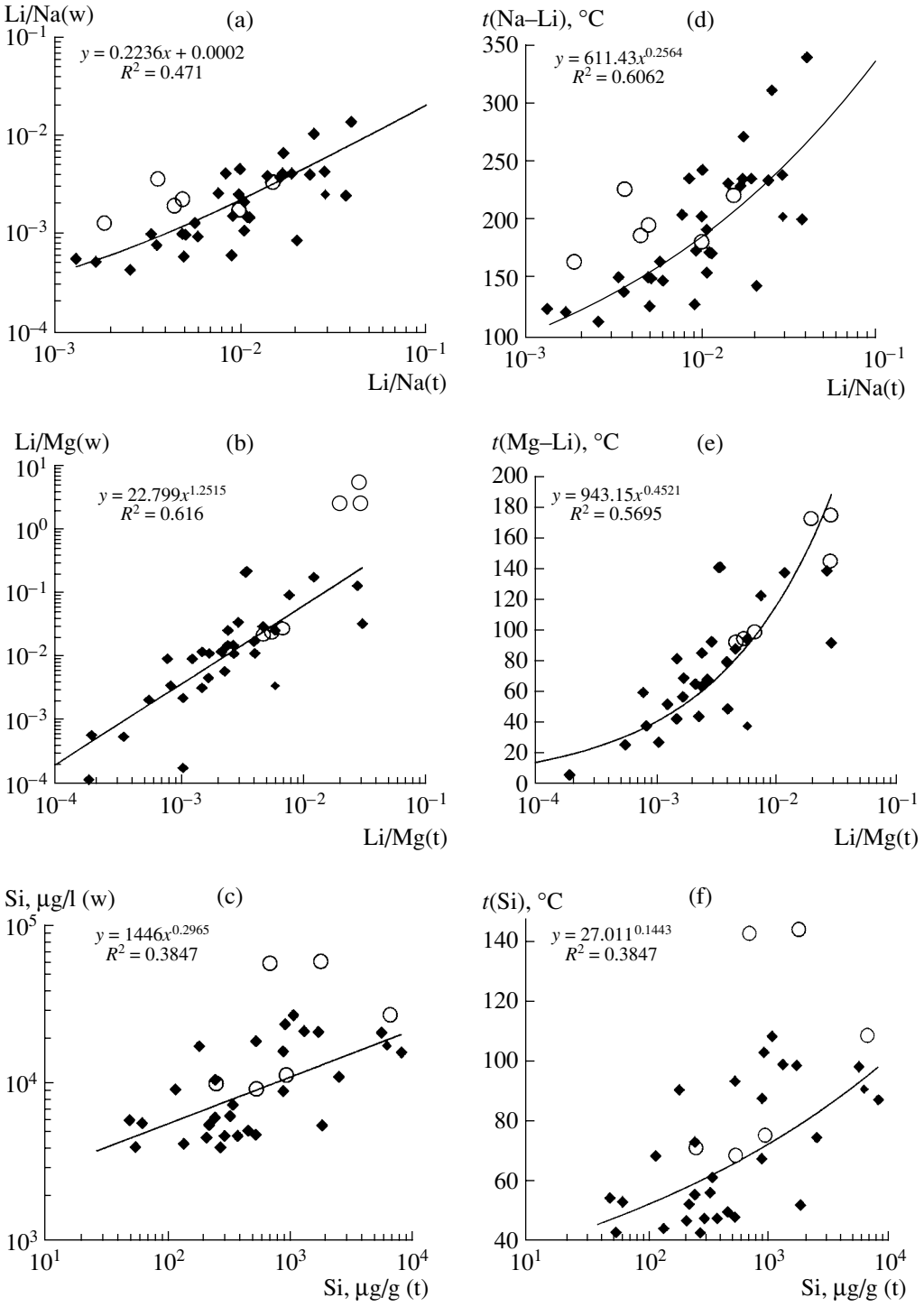

Fig. 8. Interrelations of values of (a) Li/Na, (b) Li/Mg and (c) Si concentration in travertine (t) and water (w) and their relationship with base temperatures of water formation calculated on the basis of (d) Na–Li, (e) Mg–Li, and (f) Si geothermometers. See Fig. 6 for legend.

Similar trends noted in travertine accumulations of the Yellowstone Park and Pyrenees were explained by kinetic effects of the fractionation of carbon and oxygen isotopes (Gonfiantini *et al.,* 1968; Friedman, 1970; Dandurand *et al.,* 1982).

A thermodynamic model of travertine formation was developed to test this hypothesis and appraise the scale of influence of C and O isotope fractionation on $\delta^{13}C$ and $\delta^{18}O$ values (Bychkov *et al.,* 2006). The calculations showed that the $\delta^{13}C$ value in the water–cal-

Table 5. Isotopic composition of travertines and carbonate mineralization of the Caucasus region

No. in Fig. 1	Sample no.	Spring, location of sampling	Sample description	$\delta^{13}C$, ‰ PDB	$\delta^{18}O$, ‰ SMOW
			Travertines and sinters		
			Elbrus area		
1	8-2/01	Irik-Narzan	Ferruginated travertine, middle part of dome (about 15 m downslope of spring)	5.7	22.2
1	8-4/01	Irik-Narzan	Fresh travertine, upper layer (12 m downslope of Sample 8-2/01)	5.1	21.8
1	8-3/01	Irik-Narzan	Old travertine, replacement of gruss	3.8	20.3
1	18/99	Irik-Narzan	Ferruginated travertine	5.0	20.9
1	18/99	Irik-Narzan	Travertine, dense zonal well-crystallized	4.3	19.9
2	176/99	Upper Baksan Settlement, lower narzan	Travertine, massive well-crystallized old	7.4	26.2
2	9-2/01	Upper Baksan Settlement, lower narzan	Fresh travertine (2.5 m downslope of spring), compact porous ferruginated	5.1	24.1
2	9-1/01	Upper Baksan Settlement, lower narzan	Fresh travertine, lower segment of stream (10 m downstream), scrapped from sample surface	5.4	23.3
2	9-3/01	Upper Baksan Settlement, lower narzan	Old travertine, well crystallized	5.7	26.4
2	9-5/01	Upper Baksan Settlement, lower narzan	Travertine, 3 m upslope of recent vent	7.0	27.0
26	10/01	Upper Baksan Settlement, upper narzan	Fresh travertine	6.0	24.5
26	177/99	Upper Baksan Settlement, upper narzan	Massive travertines	6.1	24.6
3	175/99	Upper Baksan Settlement, narzan, 1500 m upstream of Kyrtyk River mouth	Ferruginated travertine	5.3	22.3
4	17/99g-2	Kyrtyk River, Kyrtykaush mountain pass	Travertine in the Kyrtykaush mountain pass	6.8	23.1
4	17/99g-1	Kyrtyk River, Kyrtykaush mountain pass	Travertine in the Kyrtykaush mountain pass	6.0	23.8
5	24-1/00	Shaukol River, lower narzan	Old travertine, compact porous with sinters	7.0	23.7
6	17/98	Malka River, narzan	Travertine near the spring, compact porous fresh	6.7	25.4
6	17/98g	Malka River	Small stalactite, from a cave on the slope of Malka River valley, near narzan 17/98	6.6	25.0
7	T-2/01	Upper Tokhana Spring	Fragment of fresh travertine, 3–5 m away from spring	9.2	25.9
7	T-3/01	Upper Tokhana Spring	Travertine, fresh unbroken, 25 m away from vent	3.8	25.0
7	T-4/01	Upper Tokhana Spring	Upper layer of fresh travertine, 50 m away from vent	5.0	24.6
7	T-5/01	Upper Tokhana Spring	Upper layer of fresh travertine, 75 m away from vent	7.4	25.2
7	T-6/01	Upper Tokhana Spring	Upper layer of fresh travertine, 250 m from vent	10.0	25.8
7	T-1/01	Upper Tokhana Spring	Old travertine from dome base (about 250 m away from spring)	12.7	28.1
7	14a/98	Upper Tokhana Spring	Massive old travertine, foot of dome (about 350 m away from spring)	16.3	28.1
7	14a/98	Upper Tokhana Spring	Massive old travertine, foot of dome (about 350 m away from spring)	16.2	27.3
7	14/98	Upper Tokhana Spring	Massive, fresh travertine, middle part of dome	8.1	25.5
7	14/98	Upper Tokhana Spring	Massive travertine, middle part of dome	8.1	25.9
8	18/98	Kizilkol River, right bank	Ancient, massive travertine	7.7	23.8
9	K1/00	Kizilkol River, right bank	Travertine, ancient very dense layered (zonal)	3.9	23.1
10	K3/00	Kizilkol River, right bank	Dense old travertine	3.5	23.6
11	K4/00	Kizilkol River, right bank, well	Carbonate sinters in the casing pipe of well with CO_2-rich water	10.2	25.1
12	K5-1/00	Kizilkol River, right bank	Carbonate vein in Devonian rocks, well-crystallized calcite (Quaternary?)	6.1	25.2
12	K5-2/00	Kizilkol River, right bank	Travertine of intermediate density from old dome, 200 m upslope from K5-1/00	10.8	25.7

Table 5. (Contd.)

No. in Fig. 1	Sample no.	Spring, location of sampling	Sample description	$\delta^{13}C$, ‰ PDB	$\delta^{18}O$, ‰ SMOW
13	K6/00	Kizilkol River, right bank	Travertine, old dense well-crystallized	3.8	24.5
14	K7/00	Kizilkol River, narzan	Travertine, fresh ferruginated well-crystallized	7.4	24.5
15	4/98	Biitiktebe River, upper narzan in the riverbed	Cementation of sandy sediments in the spring area	–2.42	16.21
16	7/98	Biitiktebe River, middle reaches (about 2.5 km downstream from the Dzhilysu Spring)	Carbonate cementation of colluvium, about 30 m downslope from the center of mineral spring	5.4	22.9
17	22/01	Uchkulanichi River, upper reaches	Algal–carbonate sinters on stones near springs, intensely ferruginated	5.3	22.9
18	17/01	Amankol River	Ancient travertine (aragonite), radiate-fibrous compact well-crystallized	–1.6	24.3
19	20/00	Ingushli River, Lower Ingushli narzan	Travertine, fresh porous loose	7.2	26.0
20	7/01	Gerkhodzhan River, right tributary of the Baksan River (Tyrnyauz area)	Old travertine	1.3	24.6
			Pyatigorsk		
27	pr-00	Proval Spring, Pyatigorsk	Fresh travertine, roughly 30 m downslope from the road	6.2	19.9
27	without number	Proval Spring, Pyatigorsk	Fresh travertine, roughly 100 m downslope from the road	6.3	20.0
			Northwestern Caucasus (upper reaches of the Bol'shaya Laba River)		
28	29-2/01	Lashtrak narzan	Fresh travertine, bulk sample, upper segment of stream, 10 m downslope from spring	3.9	23.6
28	29-3/01	Lashtrak narzan	Fresh travertine, upper layer (25 m downslope from spring)	4.5	24.3
28	29-4/01	Lashtrak narzan	Fresh travertine, upper layer (35 m downslope from spring)	5.6	24.2
28	29-5/01	Lashtrak narzan	Fresh travertine, lower sample (50 m downstream from spring)	6.0	24.3
			Northern Ossetia		
29	23/99a	Tanadon River, right tributary of the Urukh River, Kubus Spring	Travertine of intermediate density, crustlike ferruginated (5 m downslope from spring)	5.3	24.6
29	23/99	Tanadon River, right tributary of the Urukh River, Kubus Spring	Travertine, ferruginated dense fresh, 10 m downslope of Sample 23/99a	6.2	24.8
30	33/00	Zrug-don River, Khasiev Spring	Travertine, compact porous, with emplacement of plant remnants	4.3	22.7
31	33-1/00	Tsmiakom-don River, right tributary of the Ardon River	Cementation of gruss with pelitomorphic carbonate	–6.4	21.4
32	35/00	Well Tib 1	Travertine sinters in casing pipe of well	4.1	21.2
33	8/03	Chel'diev narzan	Travertine, old, compact, well-crystallized (upslope of spring)	7.04	20.03
34	9/03	Karta Spring	Fresh, ferruginated travertine	7.28	21.51
35	10/03	Lower Zgil Spring	Fresh carbonate crusts	6.69	20.85
36	13/03	Bubu Spring	Fresh travertine, middle part of dome	8.77	22.15
37	38-1/00	Upper Karmadon springs	Travertine with intermediate density from spring with $T = 54$°C, upper part of dome	0.5	16.4
37	38-2/00	Upper Karmadon springs	Porous travertine from lower part of dome	0.1	18.3
38	Nar	Nar-don River	Fragment of loose travertine from alluvium, moos is replaced by pelitomorphic carbonate	–6.8	18.7

Table 5. (Contd.)

No. in Fig. 1	Sample no.	Spring, location of sampling	Sample description	$\delta^{13}C$, ‰ PDB	$\delta^{18}O$, ‰ SMOW
			Southern Ossetia		
39	18/03	Sba Spring	Sinters of old travertine	2.86	22.63
40	19/03	Suna Spring	Fresh travertine, middle part of dome	10.37	22.92
41	26/03	Lower Britata Spring (on the left bank)	Britata, old travertine dome	5.73	21.88
42	27/03	Upper Britata Spring (on right bank)	Upper Britata, fresh travertine	5.92	21.28
42	27a/03	Upper Britata Spring (on right bank)	Upper Britata, old travertine	6.33	19.74
43	28/03	Middle Britata Spring (on right bank)	Middle Britata, travertine from dry dome (poured out before earthquake)	3.51	21.88
44	31/03	Kesel'ta Spring	Carbonate veins from shales in area of mineral water vents	3.56	26.96
			Northeastern Caucasus (Dagestan)		
45	135/90	Thermal spring in channel bed flowing out from Adzhi L.	Ancient massive travertines from Novocaspian terrace	10.5	28.9
47	229/02	Andiiskoe Koisu River, Kuan narzan	Compact travertine sinters in the area of mineral water vents	4.22	27.59
48	217/02	Chakh-Chakh Spring in left tributary of Samur River	Carbonate cementation of slope deposits, 500 m downriver from the Chakh-Chakh Spring, left bank of brook	1.11	24.5
			Limestones, carbonate veins, hydrothermally altered rocks Near-Elbrus area		
22	o-1/00	Kizilkol River, alluvium	Opalite with carbonate inclusions, talus in the airfield area near the Kizilkol River	8.9	24.6
23	o-2/00	Terskol glacier, terminal moraine	Opalite with carbonate inclusions	6.6	19.4
24	without number	Biitiktebe River in area of Dzhilysu Spring	Carbonate vein in Paleozoic granite	−3.2	22.6
25	M1	Malka River (upper reaches), 2 km downstream from Dzhilysu	Fragment of Paleozoic marmorized dark gray limestone	2.0	16.4
			Northeastern Caucasus (Dagestan)		
49	D4/02	Limestone quarry in Talgi Settlement	Brown and transparent calcite crystals from carbonate–sulfide vein with inclusions of liquid oil in rock pores	2.46	22.5
49	D7/02	Limestone quarry, Talgi Settlement	Massive aragonite vein in limestones of the Talgi quarry	−13.6	17.55
49	D6/02	Limestone quarry, Talgi Settlement	Large calcite crystals, colored by bitumen, in limestone	7.23	23.49
49	D13/02	Limestone quarry, Talgi Settlement	Small calcite crystals, colored by bitumen, from fractures in limestones	6.2	23.15
49	D5/02	Limestone quarry, Talgi Settlement	Unaltered Upper Cretaceous limestones	0.96	26.04
			Taman Pen. and Eastern Georgia		
50	7/97	Eastern Georgia, Baida mud volcano	Massive calcite vein from mud breccia	−1.8	22.9
51	X/94	Taman Peninsula, Gorelyi mud volcano	Travertine from volcanic products	−8.39	25.02

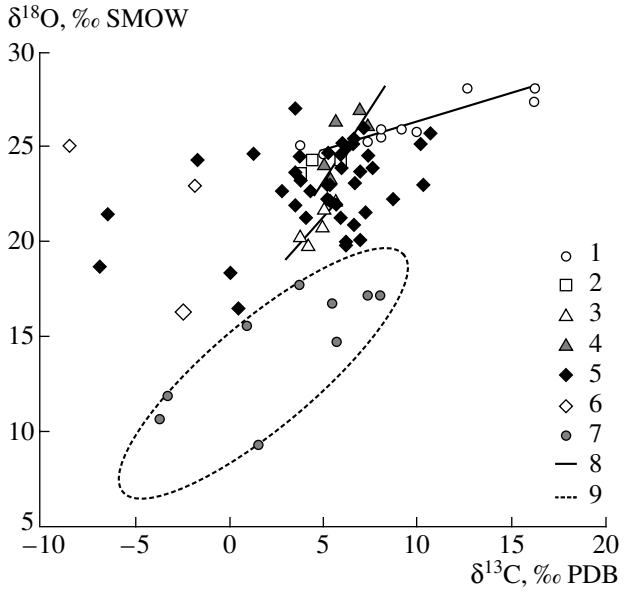

Fig. 9. Oxygen and carbon isotopes in travertines of (1–6) the Greater Caucasus and (7) eastern Chukotka. (1–4) Samples from travertine domes: (1) Upper Tokhana; (2) Lashtrak; (3) Irik-narzan; (4) Upper Baksan, lower narzan; (5) isolated samples of travertines of the Greater Caucasus; (6) carbonates from mud volcano breccia of Taman Peninsula and Georgia; (7) travertines from thermal (20–95°C) springs of eastern Chukotka (Babushkiny Ochki, Lorino, and Mechigmen springs); (8) trends for series of samples (1–4); (9) area of data points for thermal springs of eastern Chukotka.

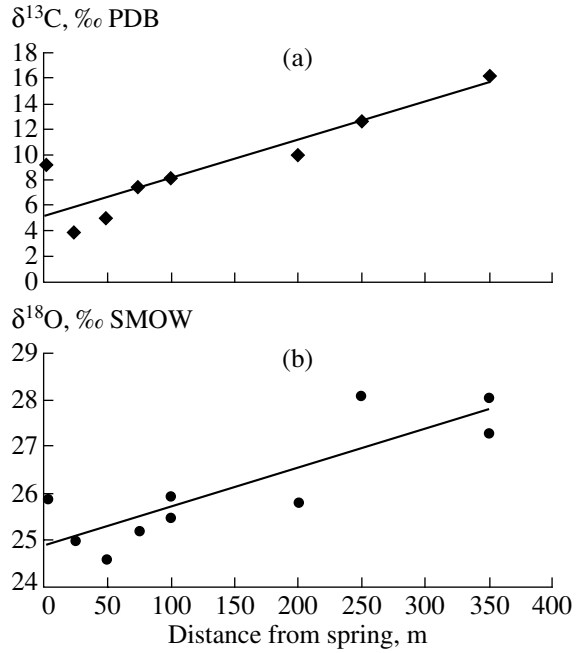

Fig. 10. Variations in (a) $\delta^{13}C$ and (b) $\delta^{18}O$ values along the strike of travertine dome from the Upper Tokhana Spring (Northern Caucasus, Elbrus area).

cite system is regulated exclusively by the process of isotope fractionation during the degassing of mineral water oversaturated with CO_2. This process dominates and significantly exceeds the role of kinetic processes accompanying the precipitation of calcite from solution.

However, this model does not render the universal explanation for the variability of $\delta^{18}O$ values. In the framework of this model, the $\delta^{18}O$ value can increase only when carbonate precipitates at low temperatures (~0°C). Considering significant altitudes (>1500–2000 m) of the majority of springs (Table 1), this probability does exist. At altitudes of more than 1500 m, the warm period (with average day temperature exceeding +5 to +10°C) lasts only 3–4 months. However, all of the springs were sampled during the warm period (July–September), and carbonate chips were taken from sample surfaces for the isotope analysis of fresh travertines, whenever possible. Therefore, such explanation is unsatisfactory.

Another process that can provoke similar changes in $\delta^{18}O$ can be water evaporation, which becomes particularly intense during summer periods and, probably, can partially or completely compensate the temperature effect of oxygen isotope fractionation in the carbonate–water system.

In general, analysis of variations in the carbonate isotopic composition in separate domes demonstrate that $\delta^{18}O$ and, particularly, $\delta^{13}C$ values can change within a wide range and increase toward the base of domes. The scale of these variations depends on the dome size. In large domes, such as Upper Tokhana, the maximal $\delta^{13}C$ ($CaCO_3$) value can reach 12.5‰.

Considering the data on other domes (Upper Baksan no. 2, Irik-narzan no. 1, and Lashtrak no. 28), the specific change of $\delta^{13}C$ along the dome strike is roughly (0.3–0.6)‰ per each 10 m. The specific change of $\delta^{18}O$ is sufficiently lower ((0.08–0.1)‰ per 10 m).

At first glance, these data show that natural variations in $\delta^{13}C$ and $\delta^{18}O$ values in the domes may be so large that they cannot be used for the reconstruction of $\delta^{13}C$ in the initial CO_2 and all the more of paleoclimatic conditions (using $\delta^{18}O$). First of all, this uncertainty concerns large travertine domes with an extent of more than 100 m. Here, carbonates from zones B and D would be the most contrasting in terms of isotopic composition. However, the bulk volume of $CaCO_3$ (~80–85 vol %) settles in Zone C, and precisely travertines from this zone are preserved for the longest period during the destruction of domes. Judging from the modeling data (Bychkov *et al.*, 2006), the range of $\delta^{13}C$ variations in travertines of the central zone (C) is significantly lower (~4‰) than in the entire dome (12.5‰).

These data give an idea about the precision of reconstruction of isotopic composition of $\delta^{13}C$ (CO_2) of fluid (apparently, not better than ±4‰ for large domes). For small domes, the precision of our estimations increases to ±2‰.

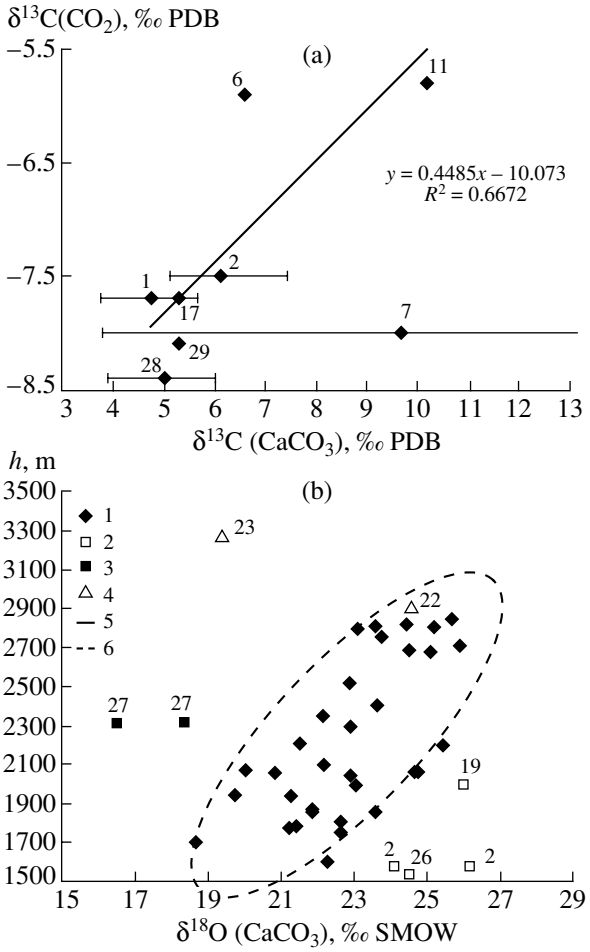

Fig. 11. Ratio of (a) $\delta^{13}C$ in travertine and spontaneous CO_2 and (b) $\delta^{18}O$ in carbonate and altitudes of spring vents. (1) Cold CO_2-rich springs; (2) springs with increased TDS content of water; (3) Upper Karmadon thermal springs; (4) opalites; (5) line of trend (except for the Upper Tokhana Spring 7 in Fig. 11a); (6) field of data points for cold CO_2-rich springs where $\delta^{18}O$ values correlate with spring altitudes. Numbers in the figure correspond to numbers of sampling sites in the first column of Table 5.

Comparison of $\delta^{13}C$ values in CO_2 and $CaCO_3$ shows that it is possible to establish the relationship between these two characteristics (Fig. 11a). However, the relationship will only be valid for small domes (with an extent of not more than 50–100 m) and cold springs.

Oxygen in travertines demonstrates a more conservative behavior, because its isotopic composition is buffered by water. The content of oxygen in water significantly exceeds the volume of ^{18}O removed from the solution by $CaCO_3$ and CO_2. Correspondingly, the $\delta^{18}O$ value depends primarily on the isotopic composition of mineral water and temperature conditions of carbonate precipitation. Indeed, carbonates precipitating in thermal springs (Upper Karmadon and Proval) are distinguished by lower $\delta^{18}O$ values (Table 5).

We do not have a sufficient number of determinations of $\delta^{18}O$ in travertine-forming springs. Therefore, interrelation between the initial isotopic composition of water and $\delta^{18}O$ ($CaCO_3$) values can only be established by an indirect way. It is known that the share of atmospheric precipitation in the feeding of CO_2-rich springs of mountain areas of the Northern Caucasus makes up no less than 95 vol % of total water (Lavrushin *et al.,* 2001a, 2003a). Thermal activity related to centers of young volcanism does not significantly affect isotope characteristics of the springs. Therefore, the isotopic signature (δD and $\delta^{18}O$) of mineral water may include traces of altitude zoning that is characteristic of atmospheric precipitation in mountain areas at different altitudes. Correspondingly, the shortage of determinations of $\delta^{18}O$ in waters of travertine-depositing springs can be supplemented to a certain extent by the data on altitudes of water vents.

Indeed, if we compare the altitudes of spring vents and $\delta^{18}O$ values in travertines, excluding thermal water flows and brackish springs at the Upper Baksan Settlement from the total sample array, the $\delta^{18}O$ versus altitude relationship can be defined by a straight line for the remaining samples (Fig. 11b).

Thus, investigation of the isotopic composition of travertines from cold springs shows that $\delta^{13}C$ and $\delta^{18}O$ values generally depend on the isotopic composition of the initial carbon dioxide ($\delta^{13}C$) and $\delta^{18}O$ value in water. However, because of kinetic effects of isotope fractionation, $\delta^{13}C$ and $\delta^{18}O$ values do not remain constant, but increase toward the base of travertine domes. In addition, the correlation of $\delta^{13}C$ and $\delta^{18}O$ values in the carbonate–water–carbonic acid system are significantly influenced by temperature conditions of carbonate precipitation. All these factors significantly lower the precision of reconstructions of the isotopic composition of initial gaseous–water fluids and sometimes make them impossible at all.

PECULIARITIES OF PALEOFLUID REGIME IN SOME AREAS OF THE GREATER CAUCASUS

For the time being, we do not have a sufficient number of different-aged samples of carbonate material in order to compile an integral image of fluid regime variations at different stages of evolution of the Greater Caucasus. The majority of sampled travertines, with the exclusion of vein deposits from the Talgi quarry (Dagestan, eastern Caucasus, no. 49) and the Elbrus area (no. 24), are located in Quaternary sediments; i.e., they are young (in most cases, Holocene). Therefore, the samples studied can only provide insights into the degree of transformation of geochemical characteristics of mineral springs in the Caucasus during the Holocene–terminal Pleistocene.

Variations in the Chemical Composition of Water in Active Springs

The tested mineral springs include some areas where travertine is not formed at present, but layers of old travertines are observed (Table 3, nos. 5, 19, 33, 39, 43, 46, and 48).

Estimations of the TDS content (based on Na and Li in travertines) show that, in many springs (Middle Shaukol no. 5, Chel'diev no. 33, Sba no. 39, and Middle Britata no. 43), the TDS content in waters, from which travertines precipitated (0.5–2 g/l), roughly corresponded to the present-day value (Table 2).

Only in a few cases, the calculated TDS content differed from the observed one. For example, estimation of the TDS content for the Lower Ingushli Spring (no. 19) shows that travertines here were formed from waters with a significantly higher TDS content (~20 g/l), relative to our sampling data (Table 2, no. 19, ~4 g/l). It is known that a highly mineralized spring (Spring no. 91, ~20 g/l) existed here until the 1930s (*Uglekislye…*, 1963). This spring was not detected during the testing in the 1950s–1990s, probably, because the vent was gradually overlapped by travertines. Thus, vents of freshened waters situated along the periphery of travertine accumulations were studied during the later testing.

Mineral spring no. 46 (Fig. 1), which appeared at the site of the emergency Nobel Well 20 (Berikei Settlement, southern Dagestan), yielded opposite values of the TDS content. Presently, brines with the TDS content of 72 g/l flow out here. Reconstruction of the salt composition shows that crusts of old travertines, which cover shores of the saline water body formed by the spring in some places, precipitated from less mineralized waters (~9 g/l). One can suppose that the sedimentary section contains several gas-saturated water reservoirs with different TDS contents and water compositions. Travertines precipitate only during the exposure of less mineralized waters, in which the gases include carbon dioxide (at present, methane predominates in the composition of spontaneous gases).

Travertines of Withered Springs and Opalites of the Elbrus Area

Mineral springs of the Elbrus area were investigated in more detail than, for example, CO_2-rich springs on the southern slope of the Greater Caucasus (Kel'sk-Kazbek region). Therefore, the majority of findings of old travertines are apparently related to the Elbrus Caldera identified on the basis of geomorphological indicators (Bogatikov *et al.,* 1998a). Samples of carbonate-bearing material are rather diverse: some samples are taken from old travertine domes on the right bank of the Kizilkol River (Table 3, nos. 9–13), while other samples represent separate fragments of travertines (Tables 3 and 5, no. 21) and hydrothermally altered volcanics (opalites) (Table 5, nos. 22 and 23) found in alluvium and terminal moraines of the Elbrus glaciers.

Six small travertine domes were found in an approximately 3-km-long sector on the right bank of the Kizilkol River valley. All of them are situated on slopes of the recent river valley and characterized by a relatively good preservation (they are not virtually affected by river erosion). Their size varies from 10–20 to 50–100 m and the thickness reaches 3–5 m. The high rate of travertine accumulation (~1–3 cm/yr) suggests that the formation of domes during a relatively short time span (100–400 yr).

Many domes are partially covered by soil. The thickness of soil cover sometimes reaches 5–10 cm. However, considering the wide distribution of colluvial sediments, it is difficult to estimate the age of domes based on the rate of soil formation. Similar modes of occurrence, degrees of the preservation of carbonate material, and patterns of soil cover suggest an almost simultaneous formation of all domes. It is probable that the synchronous formation of CO_2-rich springs in the Kizilkol River valley was related to a vigorous seismic event that revived the conduits of CO_2-rich waters. It is difficult to make any supposition about the time of their origination, but their age is likely to range from some hundreds to a few thousands of years. Probably, the onset of their formation coincides in time with the last eruption of the Elbrus Volcano dated at I–II century A.C. (Gushchenko, 1979; Bogatikov *et al.*, 1998b).

Reconstruction of the geochemical characteristics of fluids (see equations in Figs. 6 and 7) shows that travertines in the Kizilkol River valley precipitated from low-mineralized waters (0.5–2.5 g/l). Judging from low calculated concentrations of Na, Mg, S, Sr, and Ba, these waters were analogous to the present-day CO_2-rich springs in the Kizilkol, Tokhana, and Malka river valleys (*Uglekislye…*, 1963; Lavrushin *et al.,* 2001b). Reconstruction of stratal temperatures based on the Na–Li geothermometer showed that the base temperatures of waters approximately corresponded to the base temperatures (150–250°C) in the present-day springs of the Elbrus area (Lavrushin *et al.*, 2001a). According to the isotope characteristics ($\delta^{13}C$ and $\delta^{18}O$), travertines in the Kizilkol River valley (nos. 9–13) do not virtually differ from samples of fresh travertines in this region of the Caucasus (Table 5).

In terms of $\delta^{13}C$ values in $CaCO_3$, opalites taken from terminal moraines of the Elbrus Volcano (Table 5, nos. 22 and 23), are similar to recent travertines. One of the samples (no. 23) differs only by a lower $\delta^{18}O$ value, probably, indicating the precipitation of carbonates at higher temperatures. Obviously, altered volcanics (lavas) were carbonatized mainly at the final stages of fumarole activity at relatively low temperatures.

In general, analysis of the findings of old travertines in the Elbrus Volcano area shows that radical changes in isotopic and chemical compositions of gaseous–liquid fluids did not take place at least during the Holocene.

Veined and Sedimentary Carbonates

This series includes samples taken in the Elbrus area (no. 24) and northeastern Caucasus (Talgi quarry, Dagestan, no. 49). For the sake of comparison, Paleozoic and Cretaceous limestones were analyzed in both cases (Table 5, nos. 25 and 49). Samples of veined carbonates are of interest from different points of view.

The sample from a carbonate vein in Paleozoic granites taken in the Elbrus area (upper reaches of the Biitiktebe River) differs from Paleozoic travertines and limestones (Table 5, no.24) by a relatively low $\delta^{13}C$ value (–3.2‰). These data allow us to resolve the contradiction noted previously (Lavrushin *et al.*, 2001b): CO_2-rich gases in the Elbrus area are identical to gases of the upper mantle (MORB) in terms of their isotope characteristics ($\delta^{13}C$ and $^3He/^4He$ values), but they are characterized by CO_2/He values that are several orders of magnitude higher than the value in the MORB reservoir (Marty and Tolstikhin, 1998). The latter fact indicates that an additional amagmatic source of CO_2 with isotopically light composition of carbon (–7 to –5‰) participated in their formation. It is evident that Paleozoic limestones (Table 5, no. 25) can serve as such source. It is possible that precisely the thermal breakdown of veined carbonates in contact zones served as the source of the isotopically light CO_2.

Fractionation of carbon isotopes during the formation of carbonate veins can be the other possible process leading to the concentration of the isotopically light CO_2 in thermal-metamorphic gases. In this case, precipitation of calcite would be accompanied by the concentration of light carbon isotope in carbon dioxide dissolved in water.

We also studied vein mineralization in younger sediments, e.g., in Upper Cretaceous limestones in the Talgi quarry (Dagestan, northeastern Caucasus, Sample 49) (Lavrushin *et al.*, 2003c). Here, limestone massifs are crosscut by two systems of apparently different fractures. One system is filled with massive well-crystallized calcite that completely seals the fractures (Sample D7/02). The other system is filled with macrocrystalline calcite druses, whose surface is colored by oil in black-brown (samples D4/02, D6/02, and D13/02). In the second type of veins, massive aggregates of sulfides and caverns with liquid oil are also encountered.

Comparison of compositions of these carbonates shows that they were formed from sharply different fluids. Carbonates from the massive vein are distinguished by higher concentrations of Na and Li (Table 3, no. 49, Sample D7/02). Hence, they originated from waters with TDS ~2–3 g/l that are also enriched in Ba relative to Sr (Sr/Ba = 8). Calcites associated with bitumen and sulfides precipitated from waters with a lower mineralization (~0.5 g/l) and higher Sr/Ba values (34–39). In addition, fluids of both vein generations were characterized by low concentrations of SO_4 (<100 mg/l).

The base temperatures of the veined systems are also different. According to the Na–Li geothermometer, the massive vein formed from waters with a higher temperature of fluid generation (208°C) than the bitumen-bearing fluids (158–168°C). Veined deposits also sharply differ by the isotopic composition of carbonates (Table 5, no. 49, samples D6/02, D7/02, and D13/02). Calcites from the massive veins are distinguished by the lowest $\delta^{13}C$ (–13.6‰) and $\delta^{18}O$ (+17.6‰) values in comparison with other samples from the Talgi quarry.

In general, these data show that massive veins fluids were characterized by the circulation of fluids containing the isotopically light CO_2. Additionally, in contrast to carbonates impregnated with bitumen, the massive veins probably formed at higher temperatures (or from isotopically light waters). The latter fact is indirectly confirmed by the lower $\delta^{18}O$ values and higher estimates of the base temperatures.

Thus, the vein mineralization of the Talgi structure can be divided into two stages that sharply differ in terms of fluid regime (composition and temperatures of fluid generation). It is difficult to judge about their succession, because we failed to trace the relationship of veins in the section. However, we suppose that the massive (high-temperature) veins predated the bituminous ones. It is possible that they were contemporaneous with a large pluton that was emplaced at the base of the Talgi structure according to the helium isotope data (Polyak *et al.,* 2000).

CONCLUSIONS

Investigations of carbonate travertines showed that their appearance, crystalline structure, and chemical composition change along the strike of the travertine dome. The greatest variation is observed in chemical elements that precipitate together with iron hydroxides (Mn, Ni, As, Zn, Cu, Cr, V, Sc, K, P, Si, Al, REE, Th, U, Cs, Zr, Y, Be, and Ba). Rates of fixation of these elements in sediments are often different. Therefore, ratios of their concentrations can also vary along the strike of the dome (U/Th increases and Fe/Mn decreases toward the base). Hence, these elements or ratios of their concentrations are unsuitable for the reconstruction of chemical composition of fluid, on the one hand, but the trend cited above allows us to determine the direction of water movement. The latter implication can be important, for example, for the investigation of vein systems.

For other elements, e.g., REEs having similar chemical properties, concentration ratios, and pattern of distribution along the strike of the travertine dome virtually do not change. The REE spectra in travertines are analogous to their counterparts in the initial fluids. This opens perspectives for the study of REE pattern in mineral waters with the use of chemical compositions of travertines.

The travertines also include a group of elements (Na, Li, Mg, Sr, and S), concentrations of which do not virtually change along the strike of the travertine dome. Comparison of chemical compositions of travertines

and water shows that one can find correlations between the elements mentioned above that can make it possible to reconstruct their concentrations in the initial fluid. In addition, Mg/Li and Na/Li values in travertines correlate with the base temperatures based on the hydrochemical geothermometers. Hence, these data provide insights into temperature conditions of the formation of fluid system in the past.

Travertines of the Greater Caucasus differ from marine and diagenetic carbonates by higher $\delta^{13}C$ values (up to 16.3‰). The $\delta^{13}C$ and $\delta^{18}O$ values appreciably change within the dome and increase toward its base. This is dictated by kinetic effects of the fractionation of isotopes of carbon and oxygen in the water–atmosphere–calcite system. These effects are best manifested in large (>100 m) domes. Therefore, reconstruction of the isotope characteristics of fluid ($\delta^{18}O$ in H_2O and, particularly, $\delta^{13}C$ in CO_2) based on carbonate samples taken from large travertine domes or based on solitary samples from alluvium seems to have no future.

Thus, although this work is devoted to the investigation of terrestrial formations (travertines), some results presented here can likely be considered during the study of vein mineralization. First of all, this concerns the reconstruction of chemical compositions of waters and their base temperatures. Estimations of isotope characteristics ($\delta^{13}C$ and $\delta^{18}O$) of fluid systems in vein systems, obviously, must be viewed more carefully, because effects of the isotope fractionation during carbonate precipitation in this case, in contrast to travertines, are regulated not by the degassing of CO_2. A more probable mechanism is the formation of carbonate veins under the influence of other processes, such as changes of temperature in the water–rock system or mixing of waters with different chemical compositions. In this scenario, spatial variation trends of carbonate isotopic composition can be different in the vein systems. Here, in contrast to travertine domes, one should expect the decrease of $\delta^{13}C$ value along the direction of fluid movement. However, specific $\delta^{13}C$ values for these effects are difficult to estimate so far.

ACKNOWLEDGMENTS

The work was supported by the Russian Foundation for Basic Research, project nos. 00-02-64014t, 02-05-79050, and 03-05-64869.

REFERENCES

Balashov, L.S., *Geokhimiya redkozemel'nykh elementov* (Geochemistry of Rare Earth Elements), Moscow: Nauka, 1976.

Blas, V.-G., Delgado-Huertas, A., Ratto, N., and Navas, A., Large ^{13}C Enrichment in Primary Carbonates from Andean Altiplano Lakes, Northwest Argentina, *Earth Planet. Sci. Lett.*, 1999, vol. 171, pp. 253–266.

Bogatikov, O.A., Melekestsev, I.V., Gurbanov, A.G., *et al.,* The Elbrus Caldera of the Northern Caucasus, *Dokl. Akad. Nauk*, 1998a, vol. 363, no. 4, pp. 515–517 [*Dokl. Earth Sci.* (Engl. Transl.), 1998a, vol. 363, no. 9, pp. 1202–1204].

Bogatikov, O.A., Melekestsev, I.V., Gurbanov, A.G., *et al.,* Radiocarbon Dating of Holocene Eruptions of the Elbrus Volcano in the Northern Caucasus, Russia, *Dokl. Akad. Nauk*, 1998b, vol. 363, no. 2, pp. 219–221 [*Dokl. Earth Sci.* (Engl. Transl.), 1998b, vol. 363, no. 8, pp. 1093–1095].

Bychkov, A.Yu., Kostenko, O.E., Lavrushin, V.Yu., and Kuleshov, V.N., Physicochemical Model of the Formation of Isotopic Composition Carbonate Travertines in the Tokhana Spring (Elbrus Region, Northern Caucasus), *Geokhimiya*, 2006, vol. 44 (in press).

Chafetz, H., Rush, P.F., and Utech, N.M., Microenvironmental Controls on Mineralogy and Habit of $CaCO_3$ Precipitates: An Example from an Active Travertine System, *Sedimentology*, 1991, vol. 38, pp. 107–126.

Cheshko, A.L., Dubinina, E.O., Vakin, E.A., *et al.,* First Data on Hydrogen and Oxygen Isotopic Compositions in Thermal Mineral Waters of Eastern Chukotka, *Dokl. Akad. Nauk*, 2004, vol. 395, no. 5, pp. 676–680 [*Dokl. Earth Sci.* (Engl. Transl.), 2004, vol. 395A, no. 3, pp. 425–428].

Dandurand, J.L., Gout, R., Hoefs, J., *et al.,* Kinetically Controlled Variations of Major Components and Carbon and Oxygen Isotopes in a Calcite-Precipitating Spring, *Chem. Geol.*, 1982, vol. 36, no. 3/4, pp. 299–315.

Disler, V.N., Possible Evolution of CO_2-Rich Waters and N_2-Bearing Springs in Modern Orogenic Areas, *Byull. Mosk. O-va Ispyt. Prir., Otd. Geol.*, 1971, vol. 46(3), pp. 114–124.

Disler, V.N. and Avtandilova, N.I., Principles and Methods of Paleoseismic Reconstructions Based on Travertines with Reference to the Garm-Chashma CO_2-Rich Springs (Southwestern Pamirs), *Dokl. Akad. Nauk SSSR*, 1991, vol. 316, no. 3, pp. 683–687.

Disler, V.N. and Konovalova, N.I., Indicators of Formation Temperature of Travertines in the Pamirs, *Byull. Mosk. O-va Ispyt. Prir., Otd. Geol.*, 1989, vol. 50(4), no. 4, pp. 127–130.

Fouillac, C. and Michard, G., Sodium/Lithium Ratio in Water Applied to Geothermometry of Geothermal Reservoirs, *Geothermics*, 1981, vol. 10, pp. 55–70.

Fournier, R.O. and Potter, R.W., A Magnesium Correction for the Na–K–Ca Geothermometer, *Geochim. Cosmochim. Acta*, 1979, vol. 43, pp. 1543–1550.

Fournier, R.O. and Truesdell, A.H., An Empirical Na–K–Ca Chemical Geothermometer for Natural Waters, *Geochim. Cosmochim. Acta*, 1973, vol. 37, pp. 1255–1275.

Friedman, I., Some Investigations of the Deposition of Travertine from Hot Springs-I. The Isotopic Chemistry of a Travertine-Depositing Spring, *Geochim. Cosmochim. Acta*, 1970, vol. 34, no. 12, pp. 1303–1315.

Gonfiantini, R., Panichi, C., and Tongiorgi, E., Isotopic Disequilibrium in Travertine Deposition, *Earth Planet. Sci. Lett.*, 1968, vol. 5, no. 1, pp. 55–58.

Gushchenko, O.I., *Eruptions of Volcanoes in the World*, Moscow: Nauka, 1979.

Kharaka, Y.K. and Marner, R.H., Chemical Geothermometers and Their Application to Formation Waters from Sedimentary Basins, in *Thermal History of Sedimentary Basins, Methods and Case Histories*, New York: Springer, 1989, pp. 99–117.

Krainov, S.R., Rubeikin, V.Z., Kapranov, S.D., *et al.,* Specific Features of Beryllium Geochemistry in Groundwaters, *Geokhimiya*, 1966, vol. 34, no. 7, pp. 846–853.

Lavrushin, V.Yu. and Makovozov, A.O., Mineral Water Temperature as a Reflection of Magmatic Thermal Anomaly in the Kazbek Volcano Region, *Vestn. Vladikavkaz. Nauchn. Tsentr Ross. Akad. Nauk*, 2004, vol. 4, no. 3, pp. 33–40.

Lavrushin, V.Yu. and Polyak, B.G., Temperature of Mineral Waters in the Vicinity of Elbrus Volcano: Reflection of a Magmatic Thermal Anomaly, in *Geodinamika, seismotektonika i vulkanizm Severnogo Kavkaza* (Geodynamics, Seismotectonics, and Volcanism in the Northern Caucasus), Laverov, N.P., Ed., Moscow: Otd. Inst. Fiz. Zemli Ross. Akad. Nauk, 2001, pp. 241–271.

Lavrushin, V.Yu., Dubinina, E.O., Kovalenker, V.A., and Avdeenko, A.S., Genetic Features of Mineral Waters in the Elbrus Region Based on Hydrogen and Oxygen Isotopy, Abstract of Papers *XVI Simpozium po geokhimii izotopov im. akad. A.P. Vinogradova* (XVI Symposium on Isotope Geochemistry Dedicated to Academician A.P. Vinogradov, November 20–23, 2001), Moscow: Inst. Geokhim. Ross. Akad. Nauk, 2001a, pp. 139–140.

Lavrushin, V.Yu., Polyak, B.G., Pokrovskii, B.G., and Kamenskii, I.L., Evaluation of Mantle Activity in the Elbrus Region Based on the Isotopic–Geochemical Characteristics of Free Gases in Groundwaters, in *Geodinamika, seismotektonika i vulkanizm Severnogo Kavkaza* (Geodynamics, Seismotectonics, and Volcanism in the Northern Caucasus), Laverov, N.P., Ed., Moscow: Otd. Inst. Fiz. Zemli Ross. Akad. Nauk, 2001b, pp. 272–293.

Lavrushin, V.Yu., Dubinina, E.O., Avdeenko, A.S., and Kostenko, O.E., CO_2-Rich Waters of the Northern Caucasus: Origin and Formation Conditions, in *Problemy gidrogeologii XXI veka: nauka i obrazovanie* (Problems of Hydrogeology in XXI Century: Science and Education), Moscow: Ross. Univ. Druzhby Narodov, 2003a, pp. 431–433.

Lavrushin, V.Yu., Kopf, A., Deyhle, A., and Stepanets, M.I., Formation of Mud-Volcanic Fluids in Taman (Russia) and Kakhetia (Georgia): Evidence from Boron Isotopes, *Litol. Polezn. Iskop.*, 2003b, vol. 38, no. 2, pp. 147–182 [*Lithol. Miner. Resour.* (Engl. Transl.), 2003b, vol. 38, no. 2, pp. 120–153].

Lavrushin, V.Yu., Matsapulin, V.U., and Kuleshov, V.N., Paleofluid Regime of the Talgi Petroliferous Area Structure, *Tr. Inst. Geol. Dal'nevost. Nauchn. Tsentra Ross. Akad. Nauk*, 2003c, issue 49, pp. 151–153.

Marty, B. and Tolstikhin, I.N., CO_2 Fluxes from Mid-Ocean Ridges, Arcs and Plumes, *Chem. Geol.*, 1998, vol. 145, no. 3/4, pp. 233–248.

McCrea, I.M., On the Isotopic Chemistry of Carbonates and a Paleotemperature Scale, *J. Chem. Phys.*, 1950, vol. 18, no. 6, pp. 849–857.

Naboko, S.I., Lugovaya, I.P., and Zagnitko, V.N., Oxygen and Carbon Isotopic Compositions in Modern Travertines and Geyserite in Kamchatka, *Miner. Zh.*, 1999, vol. 21, no. 5/6, pp. 33–39.

Poage, M.A., Sjostrom, D.J., Goldberg, J., *et al.,* Isotopic Evidence for Holocene Climate Change in the Northern Rockies from a Goethite-Rich Ferricrete Chronosequence, *Chem. Geol.*, 2000, vol. 166, pp. 327–340.

Polyak, B.G., Lavrushin, V.Yu., Cheshko, A.L., *et al.,* The First Isotopic Study of Hydrotherms in Chukotka, Abstracts of Papers, *XVII Simpoziuma po geokhimii izotopov im. akad. A.P. Vinogradova* (XVII Symposium on Isotopic Geochemistry Dedicated to Academician A.P. Vinogradov, December 6–9, 2004), Moscow: Inst. Geokhim. Ross. Akad. Nauk, 2004, pp. 195–196.

Polyak, B.G., Tolstikhin, I.N., Yakovlev, L.E., *et al.,* Helium Isotopes, Tectonics and Heat Flow in the Northern Caucasus, *Geochim. Cosmochim. Acta*, 2000, vol. 64, no. 11, pp. 1925–1944.

Uglekislye mineral'nye vody Severnogo Kavkaza (CO_2-Rich Waters of the Northern Caucasus), Panteleev, I.Ya., Ed., Moscow: Akad. Nauk SSSR, 1963.

Zilberman, E., Amit, R., Heimann, A., and Porat, N., Changes in Holocene Paleoseismic Activity in the Hula Pull-Apart Basin, Dead Sea Rift, Northern Israel, *Tectonophysics*, 2000, vol. 321, pp. 237–252.